UNIVERSITY POLITEHNICA OF BUCHAREST

MATERIALS SCIENCE AND ENGINEERING

SUMMARY OF THESIS
FOR DOCTOR OF MATERIALS
ENGINEERING

# Surface bio-functionalization for bio-medical devices

Tran Thi Thanh
February, 2021

**Supervised by**
**Prof. Dr. M. TÂRCOLEA**

**Bucharest – 2021**

# Surface bio-functionalization for bio-medical devices

**Tran Thi Thanh**

This dissertation is proposed for a PhD degree in Materials Engineering

Faculty of Materials Science and Engineering
University POLITEHNICA of Bucharest

Approved by

**Prof. Dr. M. TÂRCOLEA**

**Advisor**

**Bucharest – 2021**

# Declaration

This work is proposed for a PhD degree of Materials Engineering at the POLITEHNICA University of Bucharest. The study was performed under the guidance of Professor Dr. Mihai TARCOLEA, period of 2015 – 2020.

This thesis is original, except where acknowledged or referenced. This research has not the similarities with any thesis which has been accepted for a degree, level, or other certificate at any university.

Parts of this work has been presented to show in the following publications:

***1. Bio-active and antibacterial coatings obtained by pulsed electrochemical deposition***, M. Tarcolea, D.M. Vranceanu, A. Vladescu, M. Dinu, T. Tran, C.M. Cotrut, 7th International Conference "Biomaterials, Tissue Engineering & Medical Devices" - BIOMMEDD'2016, 15-17 September 2016, Constanta, Romania – poster

***2. Single-step electrochemical deposition of bio-active and antibacterial coatings for medical applications***, D.M., Vranceanu, A. Vladescu, M. Dinu, T. Tran, C.M Cotrut, EMRS 2017 – Spring Meeting, 2017, 22-26 May, 2017, Strasbourg, France

***3. Pulsed electrochemical deposition of Ag doped hydroxyapatite bio-active coatings on Ti6Al4V for medical purposes***, D.M. Vraceanu, T. Tran., E. Ungureanu, V. Negoiescu, M. Tarcolea, M. Dinu, A. Vladescu, C.M. Cotrut, Scientific Bulletin U.P.B 2018, Series B - Chemistry and Materials Science, Vol. 80, Iss.1, pp. 173 – 184.

***4. Studies of micro-structure and composition of the modified HAp coating via SEM investigations***, TRAN Thi Thanh, Cosmin Mihai COTRUT, Maria Diana VRANCEANU, Elena UNGUREANU, Mihai TARCOLEA, Scientific Bulletin U.P.B 2020, Series B - Chemistry and Materials Science, Vol. 82, Iss.1, pp. 145 – 154.

***5. In vitro biocompatibility investigation of silver and zinc modified hydroxyapatite deposited on implant materials***, Thi Thanh TRAN, Norica Beatrice NICHITA, Mihaela-Olivia DOBRICA, Cosmin Mihai COTRUT, Maria Diana VRANCEANU, Mihai TARCOLEA, Scientific Bulletin U.P.B 2020, Series B - Chemistry and Materials Science, Vol. 82, Iss.3, pp. 231 – 248.

**Tran Thi Thanh**

***Bucharest, 2021***

# Content

## Surface bio-functionalization for bio-medical devices

# Chapter 1: Introduction

This research aims to investigate the micro-structure development of HAp coating on Ti and Ti6Al4V. The electrochemical deposition technique was applied to obtained pure HAp coatings, HAp-Ag coatings, HAp-Zn coatings with the requirements of micro-structure's properties, biocompatibility, bioactivity, corrosion resistance, etc.

This thesis begins, in chapter 2, with an initial recapitulation of the literature that explores our current knowledge of surface modification of Ti and Ti6Al4V via ED technique, composite coating of HAp formed by ED, Ag doped into HAp coating on Ti and Ti6Al4V, Zn doped into HAp coating on Ti and Ti6Al4V, characterization methods for HAp deposited coatings, biocompatibility test for medical devices, and corrosion test.

Chapter 3 presents the materials, methods, and equipment that the author has chosen to conduct experiments in the research process.

Chapter 4, 5, 6, 7 is devoted to the detail experiments. This section of the thesis draws together many of the topics addressed in previous chapters. The obtained results concludes that HAp coatings adapt the requirements of homogeneity, biocompatibility, bioactivity, and the ability of corrosion resistance. In addition, the author also studied the adding of silver ion ($Ag^{+}$), zinc ion ($Zn^{2+}$) into the HAp coating to explore the non-cytotoxic and biocompatible properties. The specimens were inspected by SEM technique for morphological features and EDS assessment. Surface roughness was measured by stylus profilometry over a length of 3 mm and the coatings' thickness is scanned by stylus profilometry (with stylus radius of 2.5 μm) through the edge of the coating with a length of 3 mm. Both measurements were performed on a DEKTAK 150 (Veeco Instruments, Plainview, NY, USA). Moreover, the deposited coatings were expected to more understand whether this material is in brilliant biocompatibility in conjunction with host. In this respect, the cellular actions (cells were used are HEK 293T cells) on HAp deposit on Ti (HAp/Ti), Ag doped into HAp coating on titanium (HAp-Ag/Ti), Zn doped into HAp coating on Ti (HAp-Zn/Ti) coatings was evaluated in vitro technique. The bioactivity performances of the coatings also were assessed by the immersion them in SBF solution. In addition, the electrochemical behavior was investigated at the human body temperature (37.0 ± 0.5 °C) in synthetic body fluid (SBF) with a pH value of 7.4 using a PARSTAT 4000 Potentiostat/Galvanostat.

Finally, the concluding remarks and the upcoming work orientations are mentioned by chapter 8.

# Chapter 2: Related theories

## 2.1 Surface modification of Ti and Ti6Al4V via electrochemical deposition technique

**Substrate:** Detail of steps for the substrate treatment were illustrated in [Table 2.1].

| The substrate | Treatment of the substrate | Refs |
|---|---|---|
| Ti | - Polishing with SiC paper to 400 grit<br>- Etched by the way mixed acid solution of $HNO_3$, HF and $H_2O$ for 20s, volume ratio 3:1:10<br>- Anodization in 5.0 wt..% HF, U = 20 V, within 60 min, at room temperature, Ti played as anode and Pt foil played as cathode<br>- Wash by deionized water, dry at room temperature<br>- Anneal in air at 450°C in 3h, heating rate is 15°C/min | [1] |
| | - Polishing with SiC paper from 400 grit to 1200 grit<br>- Pickling method used with 4% HF within 2 min<br>- Ultrasonic bath method was applied by series of solutions, including of acetone solution, ethyl alcohol solution, and ultrapure water in 15 minutes respectively, wash by deionized water, dry at air | [2] |
| | - Polishing with SiC paper (grit range of 400-1200)<br>- Ultrasonically by acetone, ethyl alcohol and distilled water.<br>- Etched by mixed of 3ml $HNO_3$, 1ml HF and 10 ml purified water within 20 seconds, then rinsed by purified water, after that dried in air<br>- Anodization by 5 wt..% HF solution within 60 min, U = 20 V, Ti utilized for anode and Pt foil employed as cathode<br>- Rinsed by purified water and dried in air. | [3] |
| | - Polishing with emery paper with grit range of 400- 1200<br>- Etched by the way mixed acid solution of 10% HF and 30% $HNO_3$ in 20s<br>- Ultrasonically in acetone solution and ethyl alcohol solution in 15 minutes, wash by deionized water, dry in air<br>- Anodization in 0.5 wt..% HF in room temperature, U = 20V, in 60 min, wash in deionized water and dry at air<br>- Annealed at 500°C for 2h | [4] |
| | - Polishing with SiC paper from 400 grit to 1200 grit<br>- Pickling method works with 4% HF solution within 2 min<br>- Ultrasonic bath method was applied by series of solutions acetone solution, ethyl alcohol solution, and deionized water within 15 min respectively<br>- Then dried naturally in air | [5] |
| | - Polishing with emery paper of 120 grit and 1200 grit.<br>- Anodization in 1M $H_3PO_4$, U = 180V, at room temperature | [6] |
| | - Abrade with SiC paper from 400, 600 to 1200 grit<br>- Polishing by 1 µm alumina suspension<br>- Ultrasonically by distilled water, then dry in air<br>- Anodization by electrolyte of HAp gel, U = 14.5V, for 1 day | [7] |
| | - Polishing with SiC paper from 400 grit to 1200 grit<br>- Washed by purified water, degreased by acetone, dried in air. | [8] |
| | - Etched in 12M HCl at 80°C for 1h | [9] |
| | - Wet-abraded by 600 grit SiC paper, washed out by distilled water and acetone. | [10] |
| | - Wet-abraded by 800 grit SiC paper, rinsed in a mixture of distilled water and acetone<br>- Immerse in 0.1M NaOH in room temperature for 1 day, rinse out by distilled water and drying in room temperature.<br>- Heat to 600°C in an inert atmosphere with rate 10°C/min | [11] |
| | - Abrade with SiC paper by type of 100 grit and 600 grit<br>- Pickling method with 4% HF in 2 min<br>- Ultrasonic bath method was applied by mixture of acetone solution and ethyl alcohol solution within 15 minutes, washed by purified water and dry in air | [12] |
| | - Polishing with emery paper of 300 grit and 600 grit<br>- Etched by the way mixture of HF and $HNO_3$ (volume ratio is 1:3), in 30 min, washed by purified water, then dried in air | [13] |

| | | |
|---|---|---|
| | - Anodization by electrolyte contain of 0.5M $H_3PO_4$ and 5.79g/l NaF, U = 20V, for 60 min, rinse with distilled water and dry at air | |
| | - Pickling method was applied by the way mix of HF solution, $HNO_3$ solution, and $H_2O$ with ratio is 1: 3: 10 respectively | [14] |
| Ti6Al4V | - Polishing with sandpaper, clean by a mixture of acetone solution and alcohol solution, washed in purified water, and then dry in air.<br>- Immersion in 8M NaOH at 60°C for 2 days, wash in distilled water and dry at 40°C for 1 day in an air atmosphere | [15] |
| | - Mechanically using with SiC paper (range of 600 - 1500 grit), polishing by diamond paste (type of 1.5 µm)<br>- Ultrasonically by acetone, dried<br>- Treatment with high energy electron beam, U = 700 keV, I = 1,5 mA, f = 100Hz, speed of 20m/min | [15] |
| | - Mechanical grinding, cleaned<br>- Treated by anodization for 2 min in 1M $H_2SO_4$ solution, U = 100V<br>- Soaked in NaOH solution | [17] |
| | - Mechanical grinding, grit blasting<br>- Etched in HF/$HNO_3$ solution<br>- Soaking in 5M NaOH at 60°C for 24h | [18] |
| | - Mechanical grinding and polishing with SiC paper with range of 400 - 1200 grit, wash by deionized water<br>- Ultrasonically by acetone | [19] |
| | - Abrade with abrasive paper grit of 180, wash in distilled water | [20] |

**Table 2.1 – Treatment of Ti and Ti6Al4V substrate**

### Formation of HAp coating on Ti and Ti6Al4V

Although the precursors used the ED technique to obtain the pure HAp coatings were $Ca(NO_3)_2$ and $NH_4H_2PO_4$, but in fact $Ca(NO_3)_2$ can be substituted by $Ca(NO_3)_2{\cdot}4H_2O$ or $CaCl_2$ and $NH_4H_2PO_4$ can be substituted by $K_2HPO_4$ [Table 2.2].

| Electrolyte solution | | Additive | | pH | Temperature (°C) | Solution adjusts pH | Refs |
|---|---|---|---|---|---|---|---|
| Component | Concentration (M) | Solution | Concentration (M) | | | | |
| $Ca(NO_3)_2$<br>$NH_4H_2PO_4$ | 0.042<br>0.025 | | | | | | [6] |
| $(NH_4)_2HPO_4$<br>$Ca(NO_3)_2{\cdot}4H_2O$ | | $KNO_3$ | 0.2 | 10 | | | [7] |
| $Ca(NO_3)_2{\cdot}4H_2O$<br>$K_2HPO_4$<br>0-2 wt..% Carbon nanotubes | 0.042<br>0.025 | | | 4.7 | | HCl or $NH_4OH$ | [8] |
| $CaCl_2$<br>$NH_4H_2PO_4$ | 0.167<br>0.1 | NaCl | 0.1 | 6.0 | | NaOH | [9] |
| $Ca(NO_3)_2$<br>$NH_4H_2PO_4$ | 0.042<br>0.025 | | | 4.5-5.5 | | $NaNO_3$ and $NH_3.H_2O$ | [10] |
| $CaCl_2{\cdot}2H_2O$<br>$(NH_4)_2HPO_4$ | 0.5<br>0.3 | $N_2$ | | 4.5 | 65 | HCl or $NH_4OH$ | [16] |

**Table 2.2 – Electrolyte solution for HAp coating on Ti and Ti6Al4V**

### Pulse electrochemical deposition techniques

Current research show that researchers more interested on the PED technique aim to give the HAp coatings with significantly benefits such as easy usage, elevated purity of coatings, easy alter of the experiment conditions and inexpensive cost [21-24]. The PED method permits the characterization and structures of coating might adjust and enhance by modifying factors: the on-

off cycle (it means the time for pulse on and the time for pulse off) and current density [25]. PED is a beneficial method, aim to eliminate the $H_2$ bubbles lead to enhance the adherence of HAp coatings onto substrates, this technique was detected in various reports. For example, when the pulsed current is applied, the HAp coating will be affected on the aspects such as the adhesion and crystallinity, that has been investigated at [9].

**Post-treatment**

With the alkaline method, NaOH solution with concentration in range of 0.1 – 0.25 M, at temperature in range of 60 – 80°C, the cleaning (with distilled water first and then with ultrapure water) and the drying with temperature in range of 60 – 450°C were used significantly. Thereby, the Ca-P coating would be transformed to pure HAp coating.

Heat treatments promoted as post-treatment technique for HAp coating are still investigated. This method is used to enhance the adhesion property of the HAp coatings onto the surface of the specimens.

## 2.2 Silver doped hydroxyapatite coating on Ti and Ti6Al4V substrates

| Electrolyte solution | Concentration Electrolyte solution | pH value | T (°C) | Additives | Refs |
|---|---|---|---|---|---|
| $Ca(NO_3)_2$<br>$NH_4H_2PO_4$<br>$AgNO_3$ | 0.042 mol/l<br>0.025 mol/l<br>0.1 mmol/l | 4.2 (adjusted by ammonia) | 65 | | [26] |
| $Ca(NO_3)_2$<br>$NH_4H_2PO_4$<br>$AgNO_3$ | 5.00mmol/l<br>3.00 mmol/l<br>0, 0.5 & 1 mmol/l | 4.0 (adjusted by ammonia & nitric acid) | 40 | Cysteine ($Ag^+$:cysteine = 2:1) | [27] |

**Table 2.3- The conditions of the electrolyte solution before electrodeposition process of Ag co-substituted HAp**

| Electrolyte solution | Concentration Electrolyte solution | pH value | T (°C) | Additives | Refs |
|---|---|---|---|---|---|
| $Ca(NO_3)_2$<br>$NH_4H_2PO_4$<br>$H_2O_2$<br>$AgNO_3$<br>$ZnNO_3$ | 0.49 M<br>0.29 M<br>10 ml/l<br>$10^{-3}$ M<br>$10^{-3}$ M | 4.0 – 4.5 | 70 | $H_2O_2$ | [10]. |
| $Ca(NO_3)_2$<br>$NH_4H_2PO_4$<br>$Sr(NO_3)_2$<br>$AgNO_3$ | $3.78x10^{-2}$ M<br>$2.5x10^{-2}$ M<br>$2.52x10^{-3}$ M<br>$1.68x10^{-3}$ M | 4.5 | 65 | | [11] |
| $Ca(NO_3)_2$<br>$NH_4H_2PO_4$<br>CS<br>$AgNO_3$ | 0.042 mol/l<br>0.025 mol/l<br>0.036 g/l<br>0.1 mmol/l | 4.3 (adjusted by ammonia) | 50 | | [12] |

**Table 2.4 - The conditions of the electrolyte solution before electrodeposition process of some ion co-substituted HAp.**

To obtain HAp-Ag coating, as the resource of Ag $AgNO_3$ was added into the electrolyte solution [Table 2.3]. The electrolyte solutions used for electrochemical deposition process of co-substituted HAp is presented in [Table 2.4].

### 2.3 Zinc doped into hydroxyapatite coating on Ti and Ti6Al4V

The role of Zn as a cationic substitution for Ca in apatite structures of HAp, in all most studies, the HAp-Zn coatings were obtained by using $Zn(NO_3)_2$ [28], $ZnCl_2$ [29] and $Zn(CH_3COO)_2 \cdot 2H_2O$ solutions [30].

### 2.4 Characterization method for hydroxyapatite deposited layers

- Photon-based: This technique including four method FTIR, Raman spectroscopy, X-ray and XRD.

- Microscopy techniques: This technique was operated via the microscopy, including SEM, EDX, TEM.

- Mechanical characterization techniques: This method base on the examination of mechanical property, containing Adhesion Testing, Roughness Testing, Contact angle method.

### 2.5 Biocompatibility test for medical devices: review

- In Vitro Tests for Biocompatibility: Cell culture for biocompatibility tests were used a lot of kind [Table 2.5] [31]

| Cell culture | Describe | Refs |
|---|---|---|
| L929 cell (cell of mouse, type of fibroblast cell) | - Cells were cultured in medium contains 2.0 g/L $NaHCO_3$, 4.5 g/L $C_6H_{12}O_6$, 0.11 g/L $C_3H_3NaO_3$, 2.383 g/L HEPES and 10% FBS.<br>- All cells were incubated in an incubator at environmental conditions: 37°C, 95 % air, and 5% $CO_2$.<br>- The medium was changed after each 2 days.<br>- The cells were collected by 0.25% trypsin | [37] |
| MG 63 cells (cell of human, type of osteoblast-like) | - Cell was cultured in DMEM contains 10% FBS and 40 µg/mL gentamicin<br>- 36,000 cells (density of 10,000 cells/cm$^2$) were add into 2 mL medium for each well.<br>- All cells were incubated in an incubator at environmental conditions: 37°C, 95 % air, and 5% $CO_2$ for 1, 3, and 7 days | [32] |
| MG63 (cell of human, type of osteoblasts) | - Cells were cultured in DMEM complemented with 10% FCS and 1% penicillin and streptomycin.<br>- All cells were incubated in an incubator at environmental conditions: 37°C, 95 % air, and 5% $CO_2$ | [33] |
| SD (cell of mouse, type of osteoblasts) | - Cells were cultured in a-MEM complemented with 15 % FBS<br>- All cells were incubated in an incubator at environmental conditions: 37°C, 95 % air, and 5% $CO_2$ | [27] |
| MC3T3-E1, (cell of mouse, type of calvarial cell) | - Cells were cultured in the medium contains MEM complemented with 10% FBS and 1% penicillin/streptomycin<br>- All cells were incubated in an incubator at environmental conditions: 37°C, 95 % air, and 5% $CO_2$<br>- The medium was changed after each 2 days. | [26] |
| MG63 (cell of human, type of osteoblasts) | - Cells were cultured in a medium containing of 10 ml MEM, 10% FCS, 2 mM l-glutamine, 1% penicillin/streptomycin.<br>- All cells were incubated in an incubator at environmental conditions: 37°C, 95 % air, and 5% $CO_2$<br>- The medium was changed after each 3 days. | [34] |
| MC3T3-E1, (cell of mouse, type of osteoblasts) | - Cells were cultured in α-MEM complemented with 10% FBS; and 1% penicillin/streptomycin.<br>- The cell density was 2 × 104 cells/sample.<br>- The medium was changed after each 2 days. | [35] |

**Table 2.5 – Cell culture**

- In Vivo Tests for Biocompatibility: The purpose of this experiment is to check the harm level of the medical device to the host by the evaluation of the aspects such as toxicity, genotoxicity, hemocompatibility, biodegradation, etc. [36].

**2.6 Corrosion test**

The polarization test was applied to study the corrosion behavior of coatings at $37^0$C in simulated body fluid (SBF) with electrochemical workstation. The coated or uncoated samples were the working electrode (WE) with an expose area of 1 cm2, the platinum foil (Pt) was used as the counter electrode (CE) and SCE as a reference electrode (RE), respectively. Before testing, every sample was kept in SBF until making a stable system.

**2.7 In vitro bioactivity**

The bioactivity of the coatings was investigated by studying the apatite formation ability in a simulated blood fluid (SBF) with ionic concentrations equal to human blood plasma. SBF (simulated body fluid), with pH = 7.42, was applied as a solution for the in-vitro test.

# Chapter 3: Experimental results

The results of experiments are explained in the light of the theories described in Chapter 2. As a conclusion, them can be summarized by Table 3.1

| $N_o$ | Preparation for substrate | Preparation for electrolyte | Parameter | Result |
|---|---|---|---|---|
| 3.1 Ca-P layers surfaces were obtained via electrochemical process | - Substrate: Ti6Al4V, sample shape with 2 cm of the diameter and 0.05 cm of the thickness.<br>- Mechanical polishing by PHOENIX BETA machine.<br>+ The diamond grinding disc was in size 74 µm (speed in 300 RPM, in 3 min), 15 µm (speed in 250 RPM, in 3 min).<br>+ The SiC paper with 320 and 600 grit (speed in 200 RPM, in 3 min), 800 and 1000 grit (speed in 200 RPM, in 4 min)<br>+ Micro-cloth type of 10" PSA 10/PK and Polycrystalline Diamond Polishing Suspension of 9 µm (speed in 100 RPM, in 10 min)<br>- Cleaning by the ultrasonic machine in iso-propanol alcohol for 20 min at 55°C with frequency 15kHz | - 1000 ml total volumes of 5 mM $Ca(NO_3)_2$ and 3 mM $NH_4H_2PO_4$ in distilled water.<br>- magnetic stirring stirs with a constant speed about 300 rpm during the deposition process<br>- pH = 3.990 (was adjusted by 1M $HNO_3$.<br>- $N_2$ gas was led into the electrolyte bath in 20 min<br>- Temperature: 50°C | - WE: Ti6Al4V<br>- CE: Pt<br>- RE: Ag/KCl<br>- U = -2 V to 0 V,<br>- Scan rate: 100 mV/s<br>- Break time: 100s<br>- Number of cycles: 36 | - The uniform Ca-P coating cover comparatively over specimen substrate with micro-structure flake-like morphology, which stacking to the surface of the titanium alloy substrate and forming uniformly clusters<br>- The homogeneity of Ca-P coating was assessed using the Ca/P ratio, which ranged from 0.952 to 1.699 |
| 3.2 Micro-structure and composition of HAp, HAp-Ag coating via SEM investigations | - Substrate: Ti6Al4V, place shape with 2 cm of the diameter and 0.3 cm of the thick.<br>- Mechanical polishing with SiC (300-1200 grit).<br>- Cleaning by the ultrasonic machine in acetone and water for 20 min at 55°C with the frequency 15 kHz. | - 5 mM $Ca(NO_3)_2.4H_2O$ and 3mM $NH_4H_2PO_4$<br>- 5 mM $Ca(NO_3)_2.4H_2O$, 4.5 mM $NH_4H_2PO_4$ and 0.5 mM $AgNO_3$<br>- pH = 4.0 (was adjusted by 1M $HNO_3$.<br>- magnetic stirring stirs with a constant speed about 100 rpm during the deposition process.<br>- $N_2$ gas was led into the electrolyte bath in 20 min<br>- Temperature: 75°C | - WE: Ti6Al4V<br>- CE: Pt<br>- RE: KCl<br>- U = -2 V to 0 V,<br>- Scan rate: 100 mV/s<br>- Break time: 100s<br>- Number of cycles: 36 | - The achievement of un-doped HAp coatings and doped Ag/HAp coatings obtained.<br>- HAp morphology has changed after silver doping, revealing a surface with agglomeration of spherical particle of Ag.<br>- The peaks have slightly shifted towards left, indicating that Ag is substituting the Ca present in the HAp lattice. |
| 3.3 Studies of micro-structure and composition of the HAp, HAp-Ag, and HAp-Zn coatings by SEM investigations | - Substrate: Ti, disc shape with 14 mm diameter and 1 mm thickness.<br>- Mechanical polishing with SiC (320, 600, 800 grit).<br>- Cleaning by the ultrasonic machine in 2- propanol for 20 min at 55°C with the frequency 15 kHz. | - 10 mM $Ca(NO_3)_2.4H_2O$ and 6 mM $NH_4H_2PO_4$<br>- 9.975 mM $Ca(NO_3)_2.4H_2O$, 6 mM $NH_4H_2PO_4$ and 0.025 mM $AgNO_3$<br>- 9.975 mM $Ca(NO_3)_2.4H_2O$, 6 mM $NH_4H_2PO_4$ and 0.025 mM $Zn(NO_3)_2.6H_2O$<br>- pH = 5.0<br>- magnetic stirring stirs with a constant speed about 50 rpm during the deposition process<br>- $N_2$ gas was led into the electrolyte bath in 20 min<br>- Temperature: 75°C | - WE: Ti<br>- CE: Pt<br>- RE: KCl<br>- I = 0.6 mA/cm$^2$<br>- t = 20 min | - Uniform and thick HAp, HAp-Ag, and HAp-Zn coatings were deposited successfully on a Ti surface.<br>- The microstructures of the HAp coating have been transformed from a plate-like structure to the plate-like crystals combined with white flowering branches-like structure and interconnected network-type structure.<br>- Surface roughness was found to be reduced after adding Ag and Zn elements to the HAp coating (specifically, Ra = 1847.36 nm for HAp/Ti, Ra = 482.84 nm for HAp-Ag/Ti, Ra = 214.79 nm for HAp-Zn/Ti)<br>- The thickness of the coating also decreased after adding Ag and Zn elements (specifically, HAp/Ti (12.73 µm), HAp-Ag/Ti (10.60 µm), HAp-Zn/Ti (6.20 µm) |

| | | | | |
|---|---|---|---|---|
| 3.4 Corrosion, bioactivity, and biocompatibility investigation of HAp, HAp-Ag, and HAp-Zn coatings | - Substrate: Ti, disc shape with 14 mm diameter and 2 mm thickness.<br>- Mechanical polishing with SiC (400 -, 800 grit).<br>- Cleaning by the ultrasonic machine in 2- propanol for 20 min at 55°C with the frequency 15 kHz. | - 10 mM $Ca(NO_3)_2.4H_2O$ and 6 mM $NH_4H_2PO_4$<br>- 9.975 mM $Ca(NO_3)_2.4H_2O$, 6 mM $NH_4H_2PO_4$ and 0.025 mM $AgNO_3$<br>- 9.975 mM $Ca(NO_3)_2.4H_2O$, 6 mM $NH_4H_2PO_4$ and 0.025 mM $Zn(NO_3)_2.6H_2O$<br>- pH = 5.0 (1M NaOH)<br>- magnetic stirring stirs with a constant speed about 50 rpm during the deposition process<br>- $N_2$ gas was led into the electrolyte bath in 20 min<br>- Temperature: 75°C | - WE: Ti<br>- CE: Pt<br>- RE: KCl<br>- I = - 0.85 $mA/cm^2$<br>- t = 1200 s | - The morphology of HAp was ribbon like crystals; the addition of Ag into HAp lead to some Ag particle agglomerations were noted; in the case of HAp-Zn coatings, the morphology was an interconnected porous network<br>- The elemental composition indicated that the addition of Ag and Zn enhances the Ca/P ratio of HAp from a value of 1.49 for simple HAp to 1.62 for HAp-Zn and 1.67 for HAp-Ag.<br>- After 21 days of immersion in SBF the highest values were registered for HAp-Ag coatings (7.11 mg), followed by HAp (4.58 mg) and HAp-Zn (4.38 mg), while the cp-Ti have registered the smallest value (2.11 mg);<br>. The preliminary cell culture investigations showed that Ag-HAp and Zn-HAp coating were non-cytotoxic and biocompatible and overall addition of Ag and Zn into HAp enhanced the behavior of HAp.<br>- The smallest corrosion current density and highest polarization resistance was obtained for the HAp-Zn coatings, closely followed by the ones in which Ag was used as doping element. |

**Table 3.1 - Summary of the obtained result**

## 3.1 Characterization of the calcium/phosphate layers surfaces obtained via electrochemical process

- Surface and morphological studies via SEM investigations

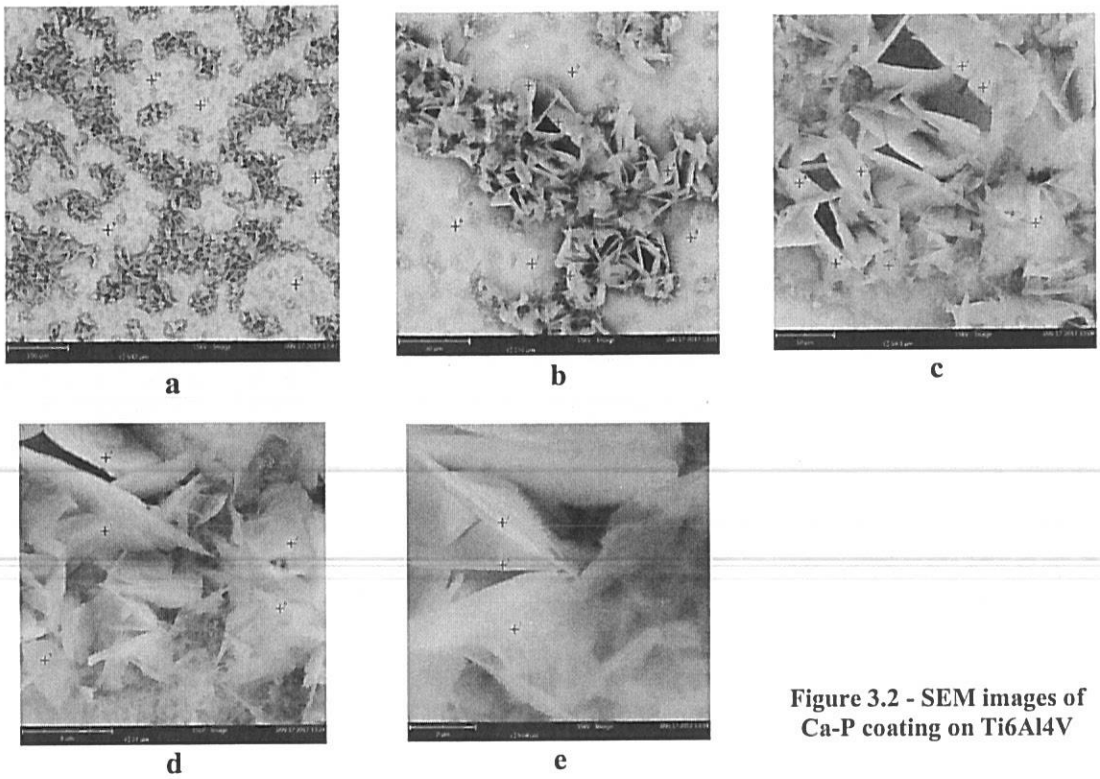


**Figure 3.2 - SEM images of Ca-P coating on Ti6Al4V**

- Composition of the deposited specimen

a

| Element Number | Element Symbol | Element Name | Atomic Conc. | Weight Conc. |
|---|---|---|---|---|
| 8 | O | Oxygen | 68.67 | 47.31 |
| 20 | Ca | Calcium | 14.17 | 24.46 |
| 15 | P | Phosphorus | 8.34 | 11.12 |
| 22 | Ti | Titanium | 7.49 | 15.43 |
| 13 | Al | Aluminium | 1.06 | 1.23 |
| 14 | Si | Silicon | 0.17 | 0.20 |
| 23 | V | Vanadium | 0.11 | 0.25 |

b

| Element Number | Element Symbol | Element Name | Atomic Conc. | Weight Conc. |
|---|---|---|---|---|
| 8 | O | Oxygen | 62.42 | 37.38 |
| 22 | Ti | Titanium | 30.28 | 54.25 |
| 13 | Al | Aluminium | 4.05 | 4.09 |
| 20 | Ca | Calcium | 1.56 | 2.34 |
| 15 | P | Phosphorus | 1.48 | 1.71 |
| 14 | Si | Silicon | 0.21 | 0.22 |

c

| Element Number | Element Symbol | Element Name | Atomic Conc. | Weight Conc. |
|---|---|---|---|---|
| 8 | O | Oxygen | 63.26 | 37.90 |
| 22 | Ti | Titanium | 29.02 | 52.02 |
| 13 | Al | Aluminium | 3.69 | 3.73 |
| 23 | V | Vanadium | 1.77 | 3.38 |
| 20 | Ca | Calcium | 1.07 | 1.60 |
| 15 | P | Phosphorus | 1.02 | 1.18 |
| 14 | Si | Silicon | 0.18 | 0.19 |

d

| Element Number | Element Symbol | Element Name | Atomic Conc. | Weight Conc. |
|---|---|---|---|---|
| 8 | O | Oxygen | 68.29 | 43.68 |
| 22 | Ti | Titanium | 23.57 | 45.11 |
| 13 | Al | Aluminium | 3.43 | 3.70 |
| 23 | V | Vanadium | 1.50 | 3.06 |
| 20 | Ca | Calcium | 1.43 | 2.30 |
| 15 | P | Phosphorus | 1.43 | 1.77 |

**Table 3.2 Elemental Composition**

a

| Element Number | Element Symbol | Element Name | Atomic Conc. | Weight Conc. |
|---|---|---|---|---|
| 8 | O | Oxygen | 73.28 | 51.84 |
| 22 | Ti | Titanium | 12.41 | 26.26 |
| 20 | Ca | Calcium | 6.77 | 11.99 |
| 15 | P | Phosphorus | 5.04 | 6.90 |
| 13 | Al | Aluminium | 2.20 | 2.62 |
| 14 | Si | Silicon | 0.31 | 0.39 |

b

| Element Number | Element Symbol | Element Name | Atomic Conc. | Weight Conc. |
|---|---|---|---|---|
| 8 | O | Oxygen | 65.07 | 42.08 |
| 22 | Ti | Titanium | 14.99 | 29.01 |
| 20 | Ca | Calcium | 10.37 | 16.81 |
| 15 | P | Phosphorus | 7.69 | 9.63 |
| 13 | Al | Aluminium | 1.44 | 1.57 |
| 23 | V | Vanadium | 0.44 | 0.91 |

c

| Element Number | Element Symbol | Element Name | Atomic Conc. | Weight Conc. |
|---|---|---|---|---|
| 8 | O | Oxygen | 54.02 | 31.56 |
| 22 | Ti | Titanium | 18.42 | 32.19 |
| 20 | Ca | Calcium | 14.64 | 21.43 |
| 15 | P | Phosphorus | 10.88 | 12.31 |
| 13 | Al | Aluminium | 1.48 | 1.46 |
| 23 | V | Vanadium | 0.56 | 1.05 |

d

| Element Number | Element Symbol | Element Name | Atomic Conc. | Weight Conc. |
|---|---|---|---|---|
| 8 | O | Oxygen | 70.10 | 48.75 |
| 20 | Ca | Calcium | 11.40 | 19.86 |
| 22 | Ti | Titanium | 8.90 | 18.52 |
| 15 | P | Phosphorus | 8.62 | 11.61 |
| 13 | Al | Aluminium | 0.85 | 1.00 |
| 23 | V | Vanadium | 0.12 | 0.26 |

e

| Element Number | Element Symbol | Element Name | Atomic Conc. | Weight Conc. |
|---|---|---|---|---|
| 8 | O | Oxygen | 66.19 | 44.20 |
| 20 | Ca | Calcium | 13.08 | 21.88 |
| 22 | Ti | Titanium | 9.75 | 19.47 |
| 15 | P | Phosphorus | 9.67 | 12.50 |
| 13 | Al | Aluminium | 0.84 | 0.95 |
| 23 | V | Vanadium | 0.47 | 1.00 |

**Table 3.3 Elemental Composition**

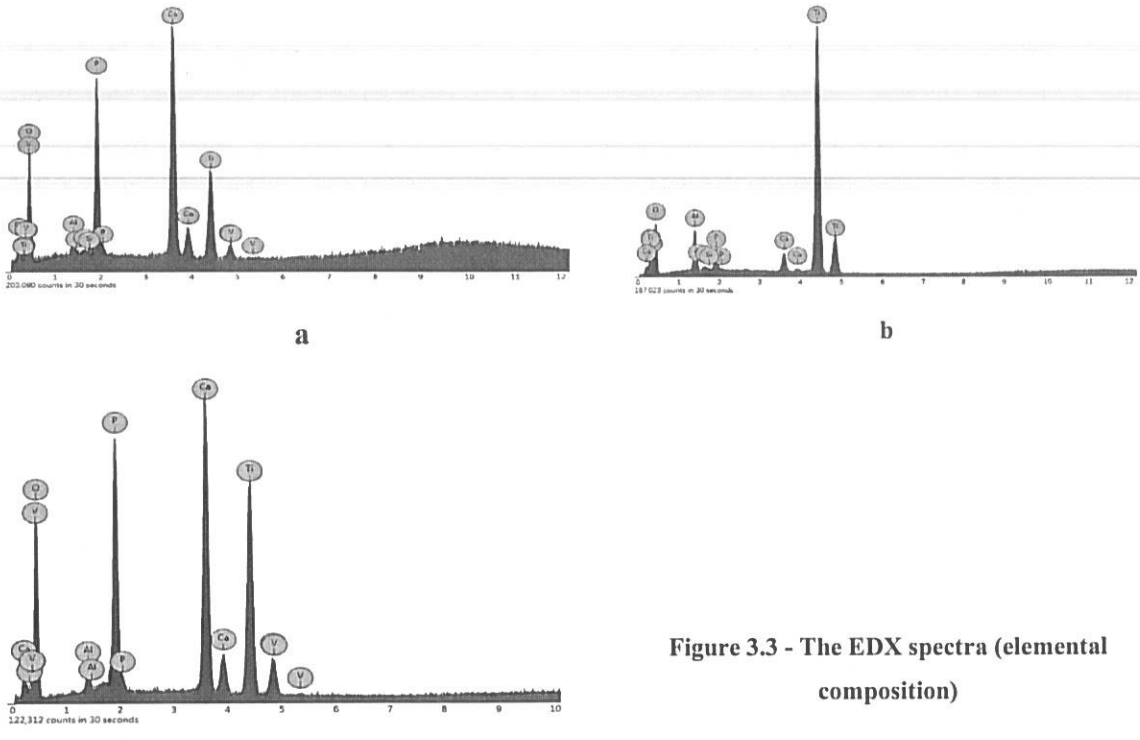


**Figure 3.3 - The EDX spectra (elemental composition)**

### 3.2 Micro-structure and elemental composition of HAp, HAp-Ag coatings

- Micro-structure of coatings studies

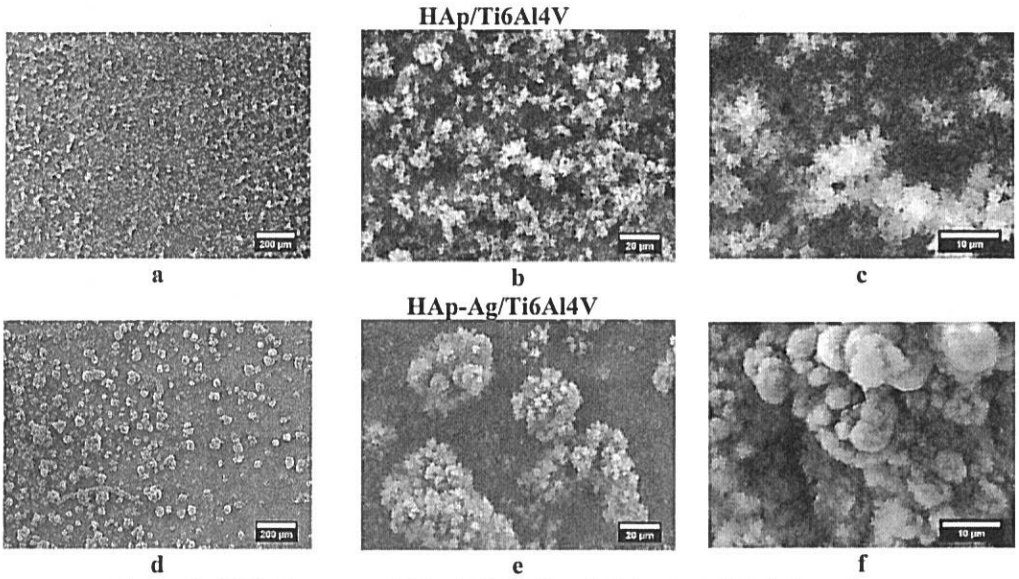


**Figure 3.4 SEM images of HAp/Ti6Al4V and HAp-Ag/Ti6Al4V coatings**

- The elemental composition analysis

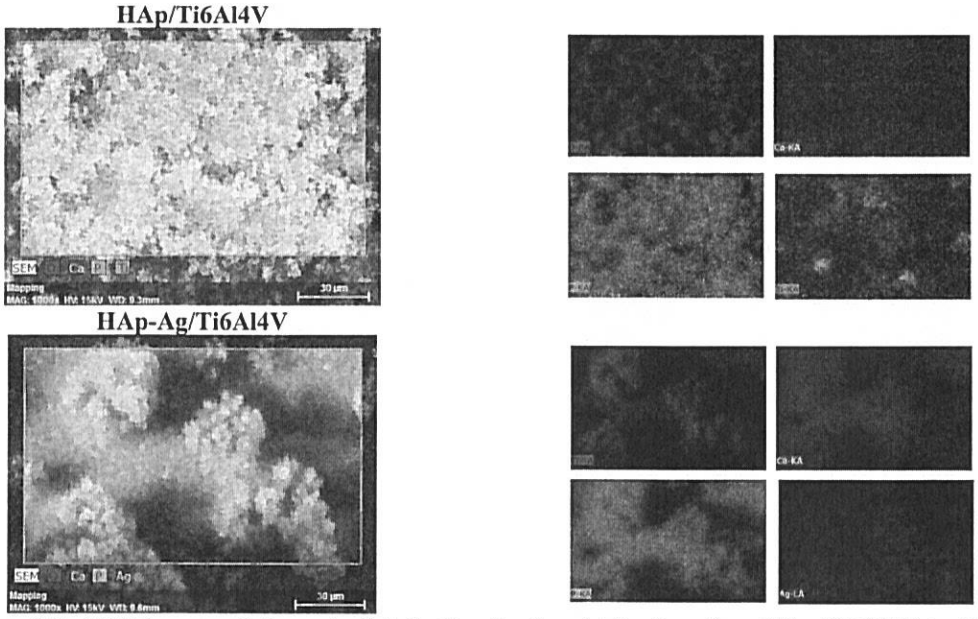


**Figure 3.5 - SEM images of elements distribution for the obtained coatings HAp/Ti6Al4V (a, b) and HAp-Ag/Ti6Al4V (c, d)**

| Sample | HAp/Ti6Al4V | | | | HAp-Ag/Ti6Al4V | | | |
|---|---|---|---|---|---|---|---|---|
| Elemental composition | Area 1 | | Area 2 | | Area 1 | | Area 2 | |
| | % wt. | % at | % wt.. | % at | % wt. | % at | % wt. | % at |
| Ca | 38.04 | 21.80 | 38.03 | 21.69 | 34.55 | 21.19 | 33.31 | 19.40 |
| P | 15.77 | 11.70 | 15.29 | 11.29 | 14.86 | 11.79 | 14.53 | 10.95 |
| O | 42.14 | 60.51 | 42.59 | 60.86 | 39.53 | 60.72 | 42.97 | 62.70 |
| Ti | 1.23 | 0.59 | 1.13 | 0.54 | - | - | - | - |
| C | 2.82 | 5.39 | 2.95 | 5.62 | 2.87 | 4.25 | 2.87 | 5.58 |
| Ag | - | - | - | - | 8.98 | 2.05 | 6.32 | 1.37 |
| Ca/P ratio | *1.86* | | *1.92* | | *1.97* | | *1.90* | |

**Table 3.4- Elemental composition of the obtained coatings examined by EDS**

- The phase composition of the coatings

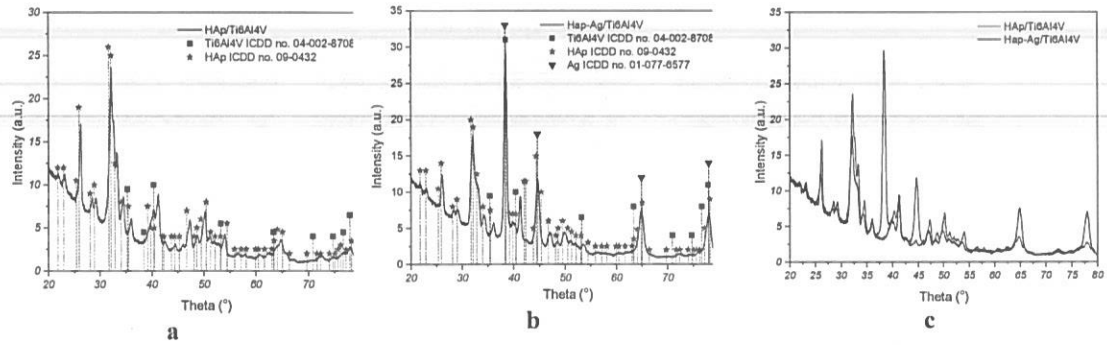


**Figure. 3.6 - XRD pattern of the obtained coatings a) HAp/Ti6Al4V, b) HAp-Ag/Ti6Al4V, c) their overlay**

## 3.3 Studies of microstructure and composition of HAp, HAp-Ag, and HAp-Zn coatings

- Morphological investigation

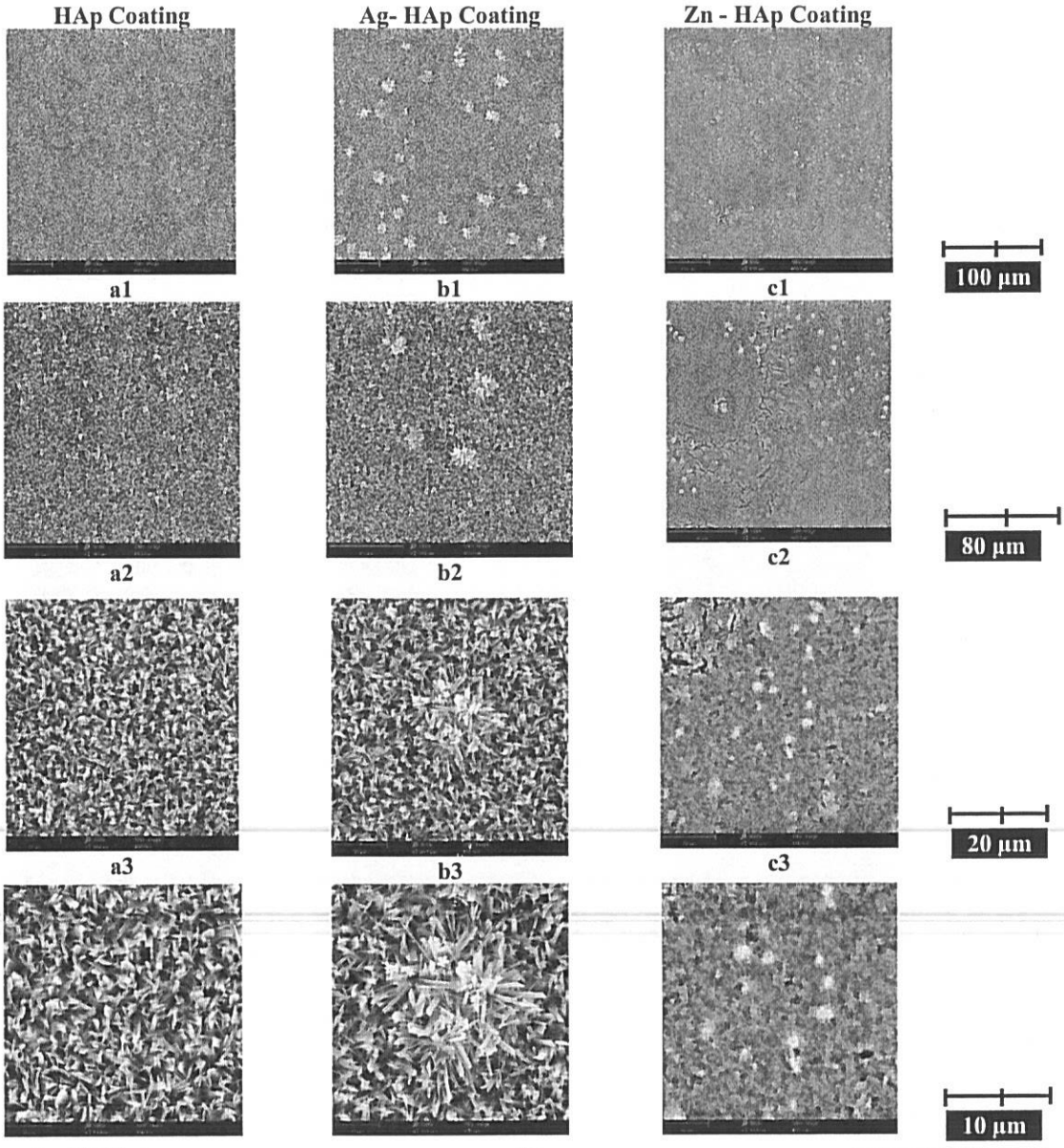

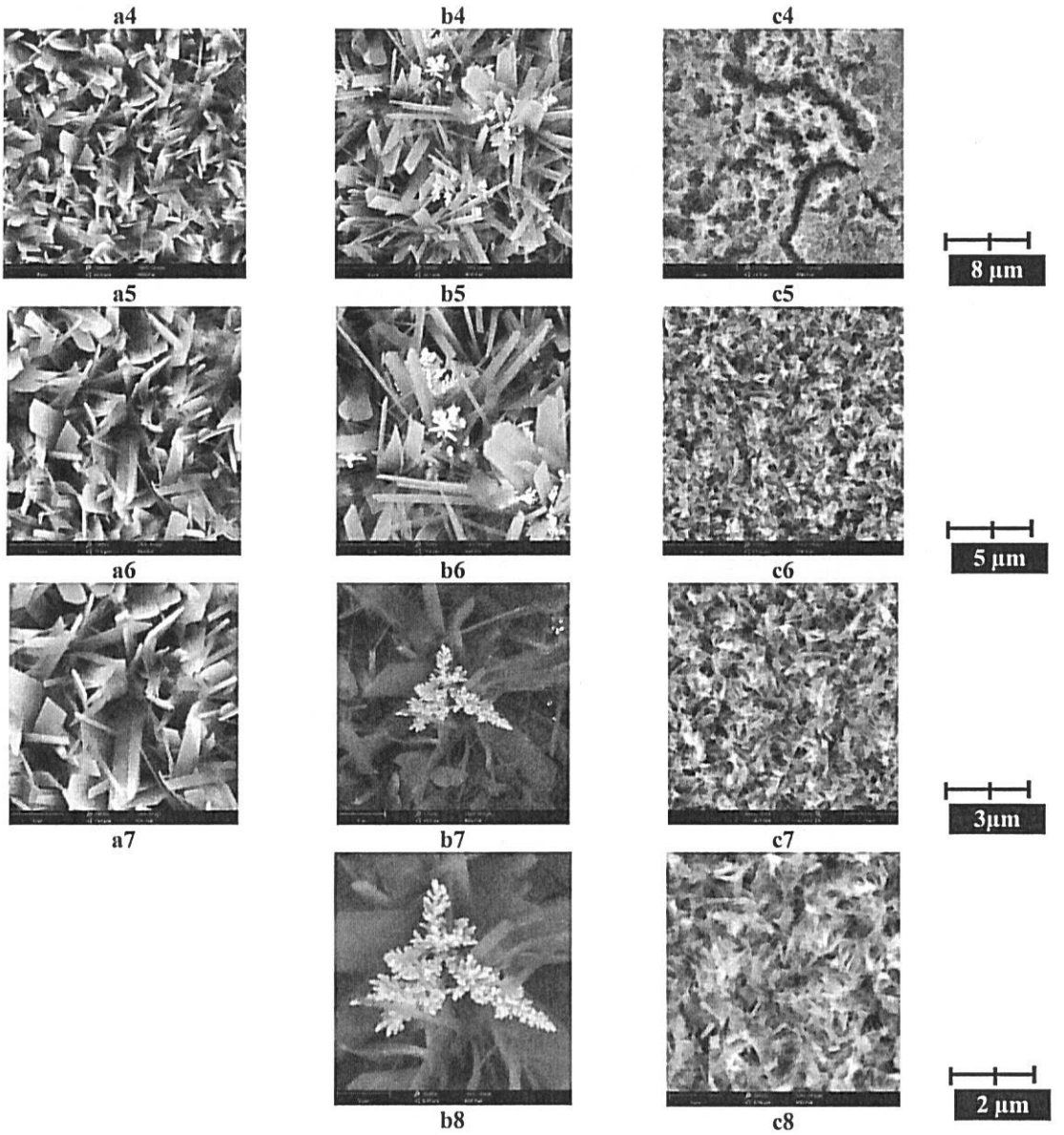


**Figure 3.7 - SEM micrograph of the HAp, HAp-Ag, HAp-Zn coatings obtained using electro-deposition at magnifications ×500 (a1, b1 c1), ×1000 (a2, b2, c2), × 3000 (a3, b3, c3), ×5000 (a4, b4, c4), ×10000 (a5, b5, c5), ×15000 (a6, b6, c6), ×25000 (a7, b7, c7), ×30000 (b8, c8)**

- Elemental composition

| Coating | HAp/Ti | | HAp-Ag/Ti | | | | HAp-Zn/Ti | | | |
|---|---|---|---|---|---|---|---|---|---|---|
| Elemental composition | Area 1 | | Area 2 | | Area 3 | | Area 6 | | Area 4 | |
| | % wt. | % at | % wt. | % at | % wt. | % at | % wt. | % at | % wt. | % at |
| Ca | 32.09 | 18.10 | 60.22 | 58.89 | 65.67 | 60.70 | 67.21 | 61.41 | 66.91 | 61.35 |
| P | 16.83 | 12.28 | 29.55 | 37.39 | 32.27 | 38.59 | 32.51 | 38.43 | 32.12 | 38.11 |
| O | 48.38 | 68.35 | - | - | - | - | - | - | - | - |
| Ti | 2.70 | 1.27 | - | - | - | - | - | - | - | - |
| Ag | - | - | 10.24 | 3.72 | 2.07 | 0.71 | - | - | - | - |
| Zn | - | - | - | - | - | - | 0.29 | 0.16 | 0.98 | 0.55 |
| Ca/P ratio | *1.47* | | *1.67* | | *1.94* | | *1.60* | | *1.62* | |

**Table 3.5 - Elemental composition of the obtained coatings by electrochemical deposition**

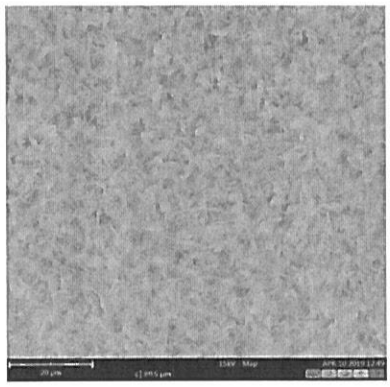

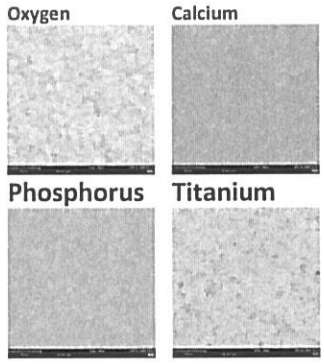


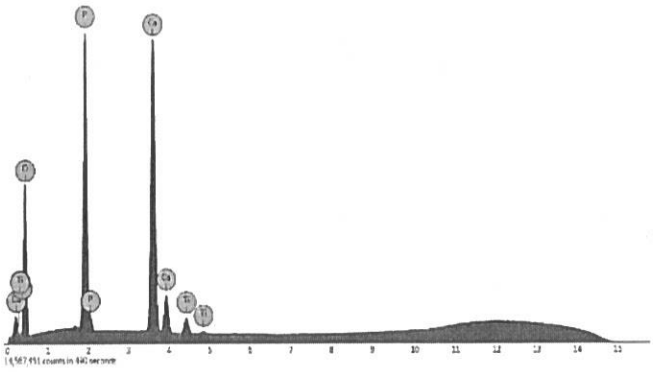

| Element Number | Element Symbol | Element Name | Atomic Conc. | Weight Conc. |
|---|---|---|---|---|
| 8 | O | Oxygen | 68.35 | 48.38 |
| 20 | Ca | Calcium | 18.10 | 32.09 |
| 15 | P | Phosphorus | 12.28 | 16.83 |
| 22 | Ti | Titanium | 1.27 | 2.70 |

**Figure 3.8 a - Chemical composition and elemental distribution for HAp/Ti coatings examined by EDS elemental mapping**

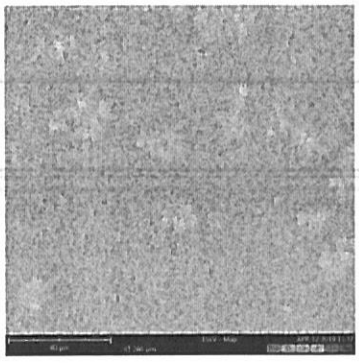

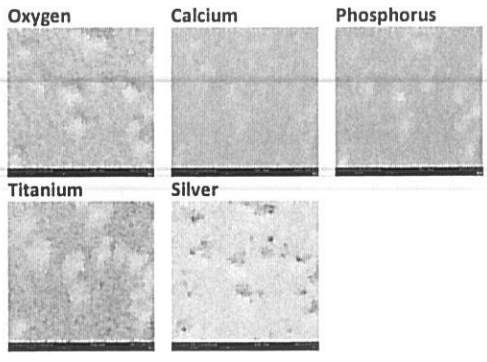

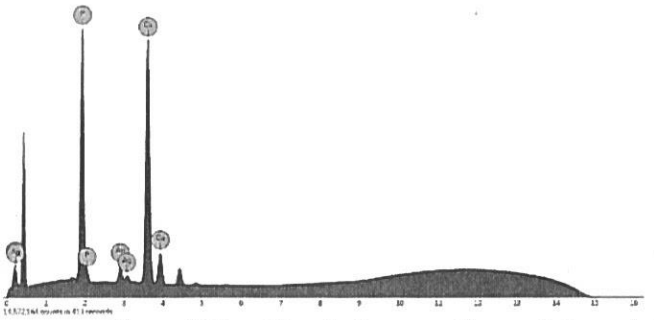

| Element Number | Element Symbol | Element Name | Atomic Conc. | Weight Conc. |
|---|---|---|---|---|
| 20 | Ca | Calcium | 58.89 | 60.22 |
| 15 | P | Phosphorus | 37.39 | 29.55 |
| 47 | Ag | Silver | 3.72 | 10.24 |

**Figure 3.8 b - Chemical composition and elemental distribution for HAp-Ag/Ti coatings examined by EDS mapping**

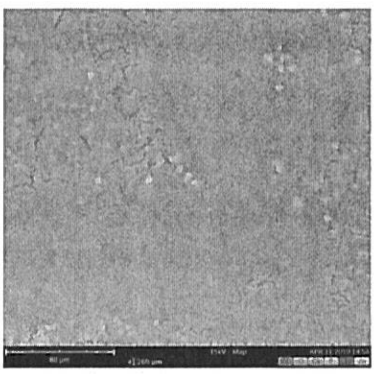

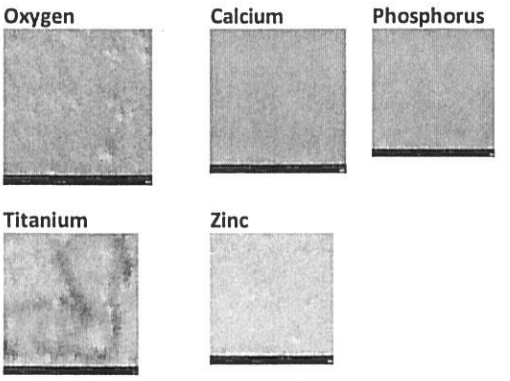


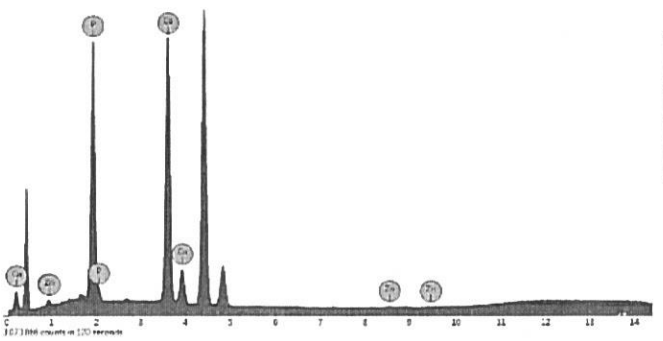

| Element Number | Element Symbol | Element Name | Atomic Conc. | Weight Conc. |
|---|---|---|---|---|
| 20 | Ca | Calcium | 61.35 | 66.91 |
| 15 | P | Phosphorus | 38.11 | 32.12 |
| 30 | Zn | Zinc | 0.55 | 0.98 |

**Figure 3.8 c - Chemical composition and elemental distribution for HAp-Zn/Ti coatings examined by EDS elemental mapping**

## The surface roughness

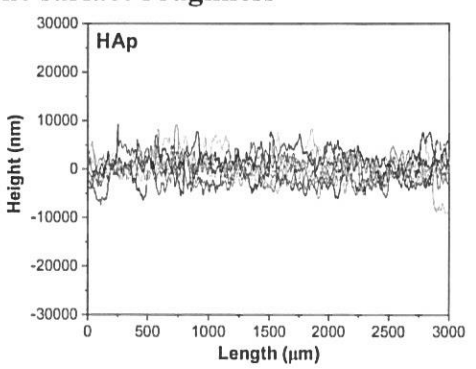


a

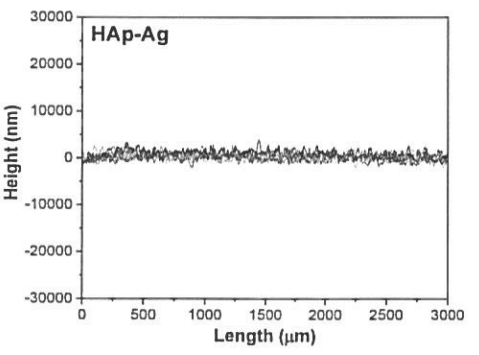


b

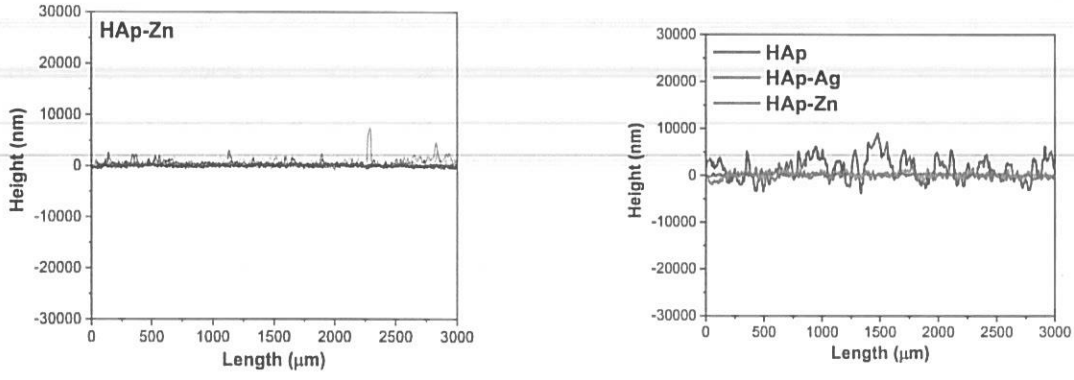


c d

**Figure 3.9 - Profile lines specific for each group surface (a-c) and d) overlap of representative profile lines specific for each material**

| Samples | Ra (nm) | *SD* | Rq (nm) | *SD* | Skew | *SD* |
|---|---|---|---|---|---|---|
| HAp | 1847.36 | *± 277.07* | 2258.69 | *± 303.65* | 0.50 | *± 0.23* |
| HAp-Ag | 482.84 | *± 35.17* | 608.72 | *± 43.75* | 0.17 | *± 0.10* |
| HAp-Zn | 214.79 | *± 46.31* | 278.65 | *± 63.96* | 0.82 | *± 0.25* |

**Table 3.6 - Characteristic roughness parameters**

**(Ra-average roughness, Rq-root mean square, Skew-skewness)**

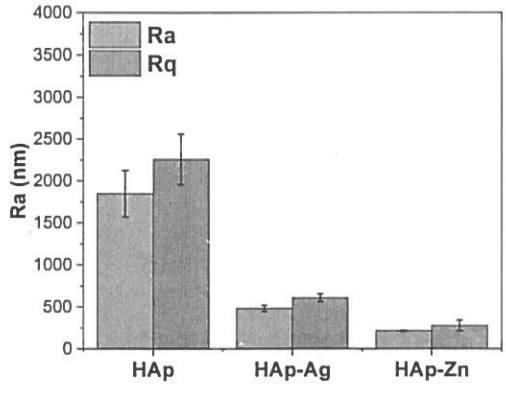


**Figure 3.10 - Coating roughness (Ra and Rq)**

## The coating thicknesses

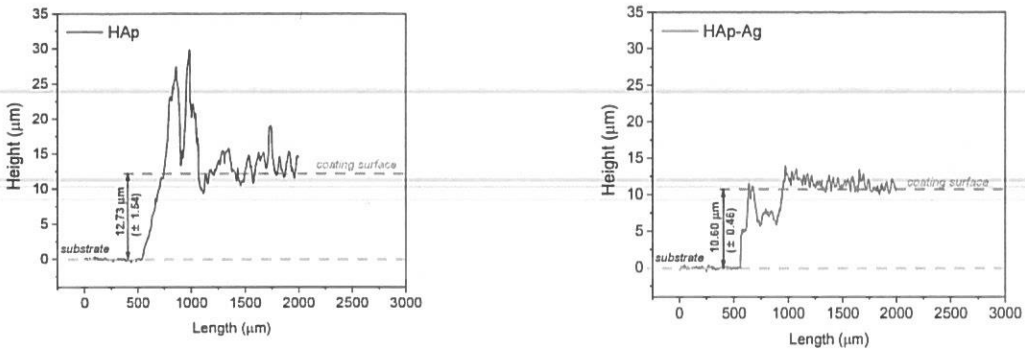

a b

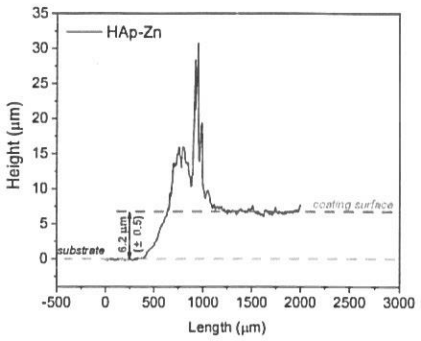


c

**Figure 3.10 - Coating thickness of HAp/Ti (a), HAp-Ag/Ti (b), and HAp-Zn/Ti (c) coatings**

| Samples | Thickness (µm) | SD |
|---|---|---|
| HAp | 12.73 | ± *1.54* |
| HAp-Ag | 10.60 | ± *0.46* |
| HAp-Zn | 6.20 | ± *0.51* |

**Table 3.11 - Coating thickness of HAp/Ti (a), HAp-Ag/Ti (b), and HAp-Zn/Ti (c) coatings**

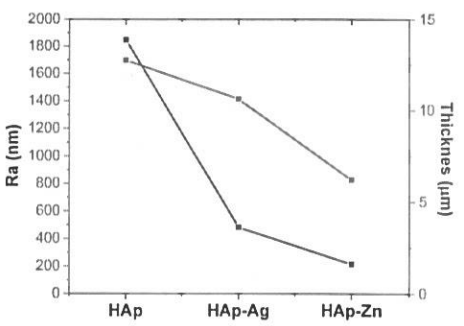


**Figure 3.12 - Dependency between the roughness (Ra) and thickness values of the investigated coatings**

## 3.4 Corrosion, bioactivity, and biocompatibility investigation of HAp, HAp-Ag and HAp-Zn coatings

- Evaluation of Bioactivity

| Sample | Mass [mg] | | | | |
|---|---|---|---|---|---|
| | Day 1 | Day 3 | Day 7 | Day 14 | Day 21 |
| cp-Ti | 0.01 (±0.01) | -0.01 (±0.01) | 0.01 (±0.01) | 0.01 (±0.01) | 2.62 (±0.01) |
| HAp | 0.51 (±0.01) | 0.71 (±0.01) | 1.19 (±0.01) | 2.08 (±0.01) | 4.58 (±0.01) |
| HAp-Ag | 0.41 (±0.01) | 1.25 (±0.01) | 2.59 (±0.01) | 3.60 (±0.01) | 7.11 (±0.01) |
| HAp-Zn | 0.17 (±0.01) | 1.11 (±0.01) | 2.48 (±0.01) | 3.41 (±0.01) | 4.38 (±0.01) |

**Table 3.8 - Mass evolution of the newly apatite layer on substrate after immersion in SBF**

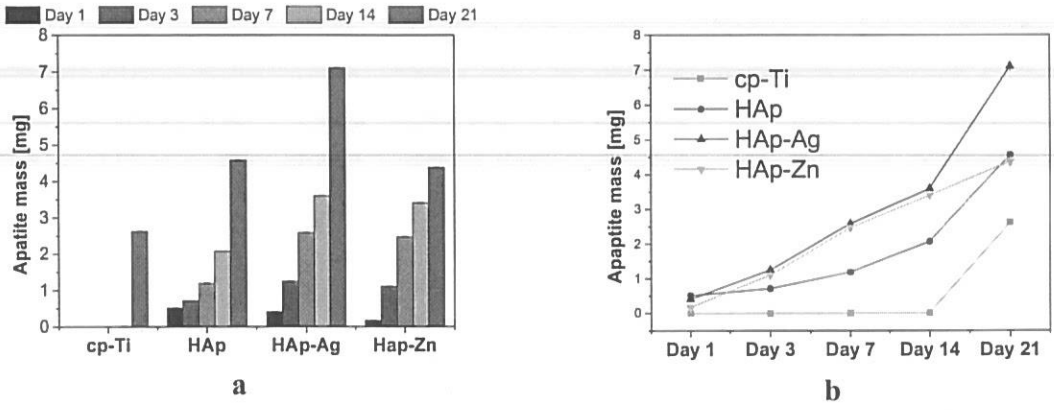


**Figure 3.13 - The chart shows the increase in the mass of the apatite layer on Ti**

- Electrochemical corrosion analysis

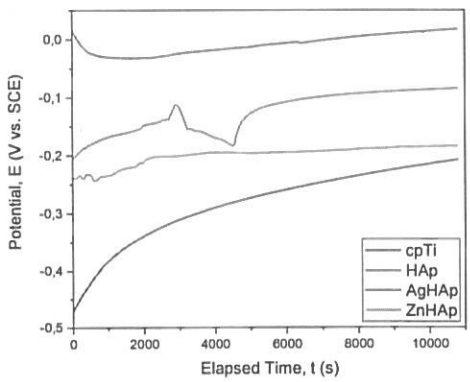


**Figure 3.14 - Open circuit potential of cp-Ti and HAp coatings**

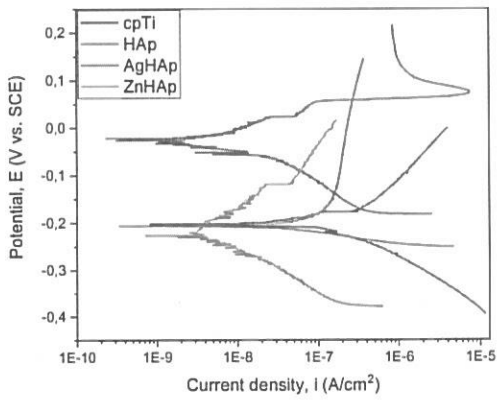


**Figure 3.15 -Tafel plots of cp-Ti and HAp coatings**

| Nr.crt. | Sample | $E_{oc}$ (mV) | $E_{corr}$ (mV) | $i_{corr}$ (nA/cm²) | $\beta_c$ (mV) | $\beta_a$ (mV) | Rp (kΩxcm²) |
|---|---|---|---|---|---|---|---|
| 1 | cp Ti | -209.50 | -201.25 | 246.15 | 112.12 | 160.20 | 116.50 |
| 2 | HAp | -82.45 | -207.21 | 128.40 | 45.24 | 777.85 | 144.78 |
| 3 | HAp-Ag | 18.54 | -18.48 | 9.12 | 94.87 | 64.12 | 182.35 |
| 4 | HAp-Zn | -184.02 | -225.99 | 7.91 | 107.63 | 175.42 | 366.33 |

**Table 3.9 - Main electrochemical parameters**

- Evaluation of biocompatibility

+ Cell morphology

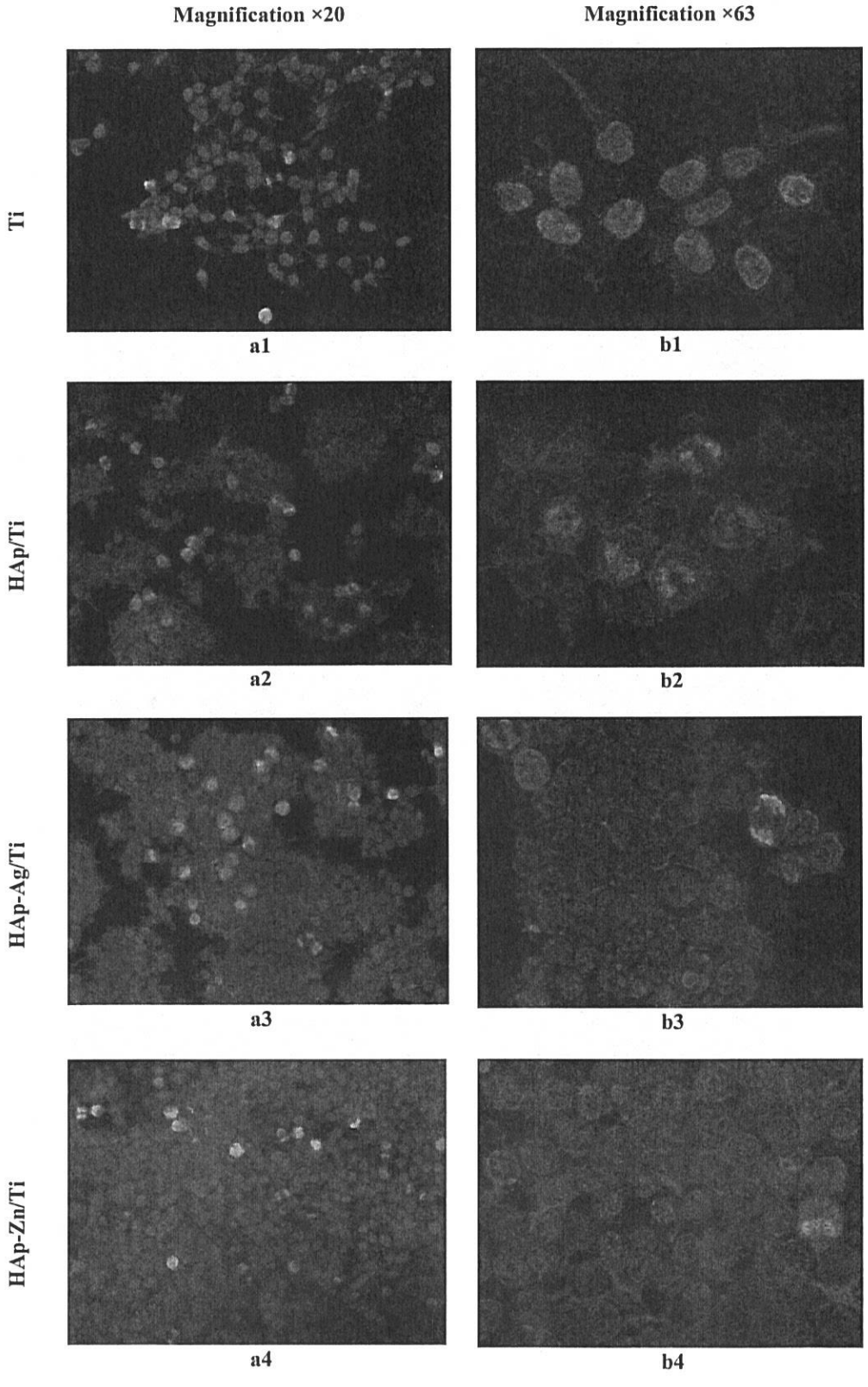


**Figure. 3.16 - The results of staining for Actin and Ki67 of the HEK 293T cells (Actin-red, Ki67-green)**

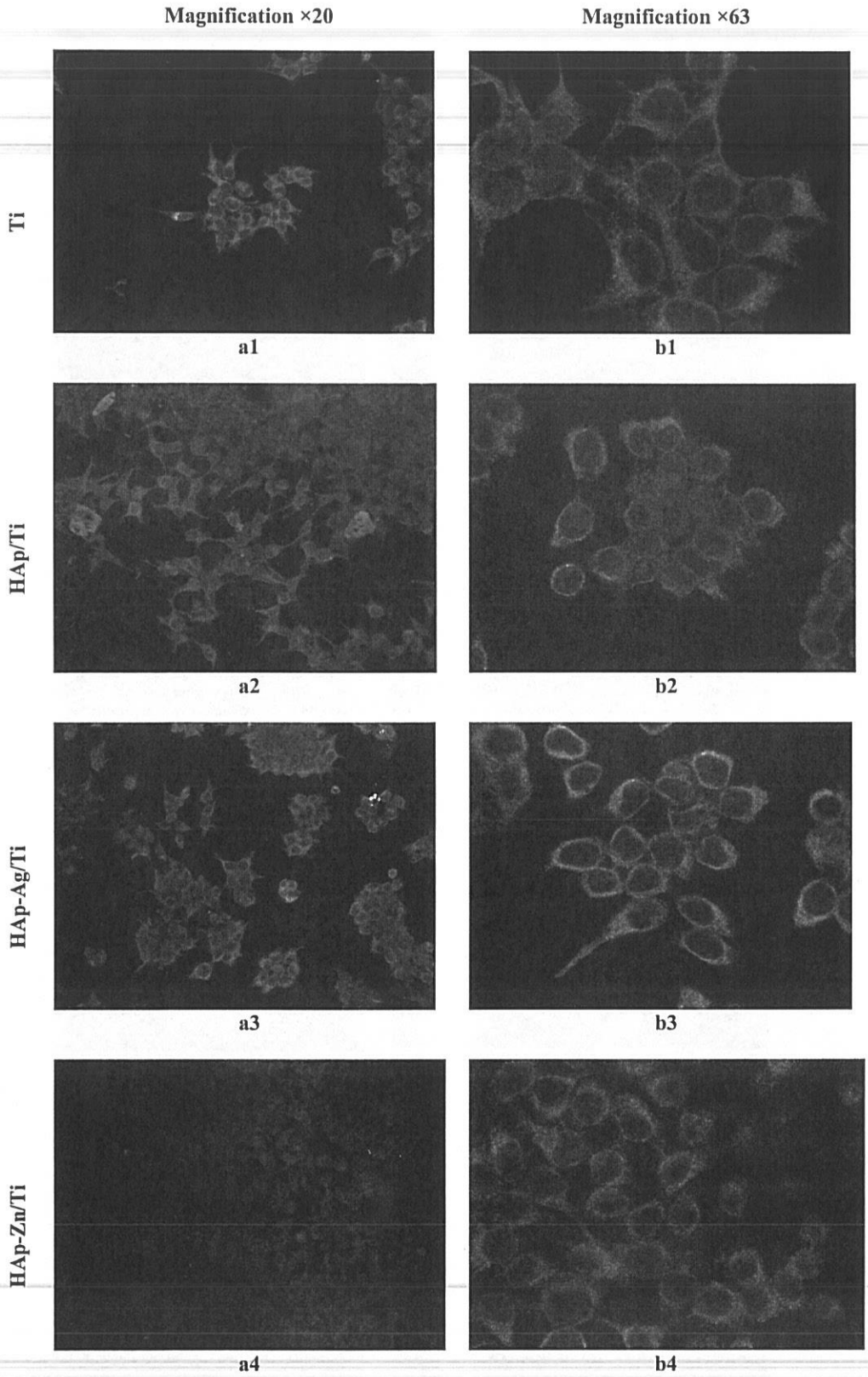


**Figure 3.17 - The results of staining for Tubulin and PDI of the HEK 293T cells (Tubulin-red, PDI-green)**

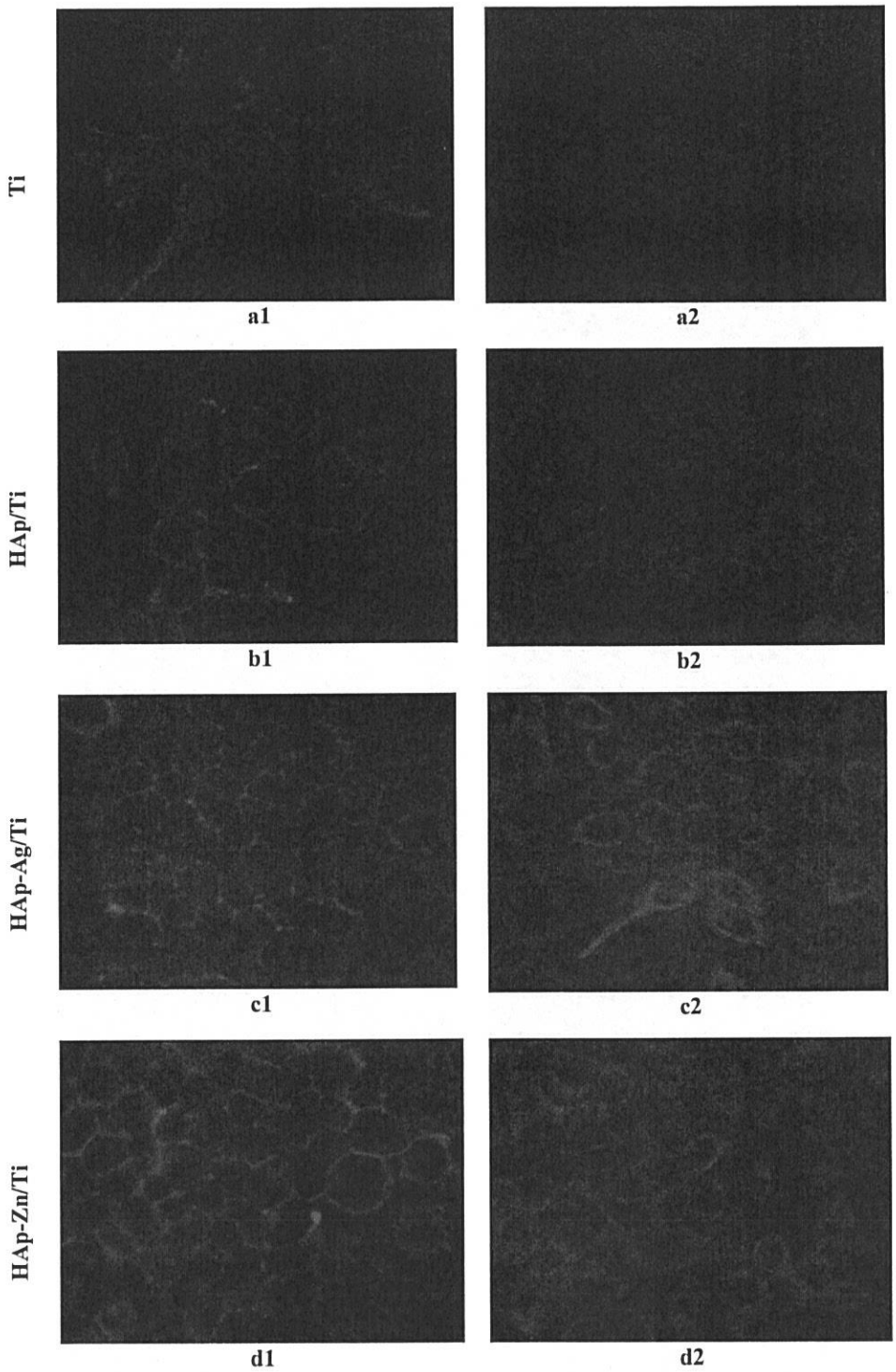


**Figure 3.18a - Staining for Actin of the coating at magnification ×63 (a1, b1, c1, d1)**

**Figure 3.18b - Staining for Tubulin of the coating at magnification ×63 (a2, b2, c2, d2)**

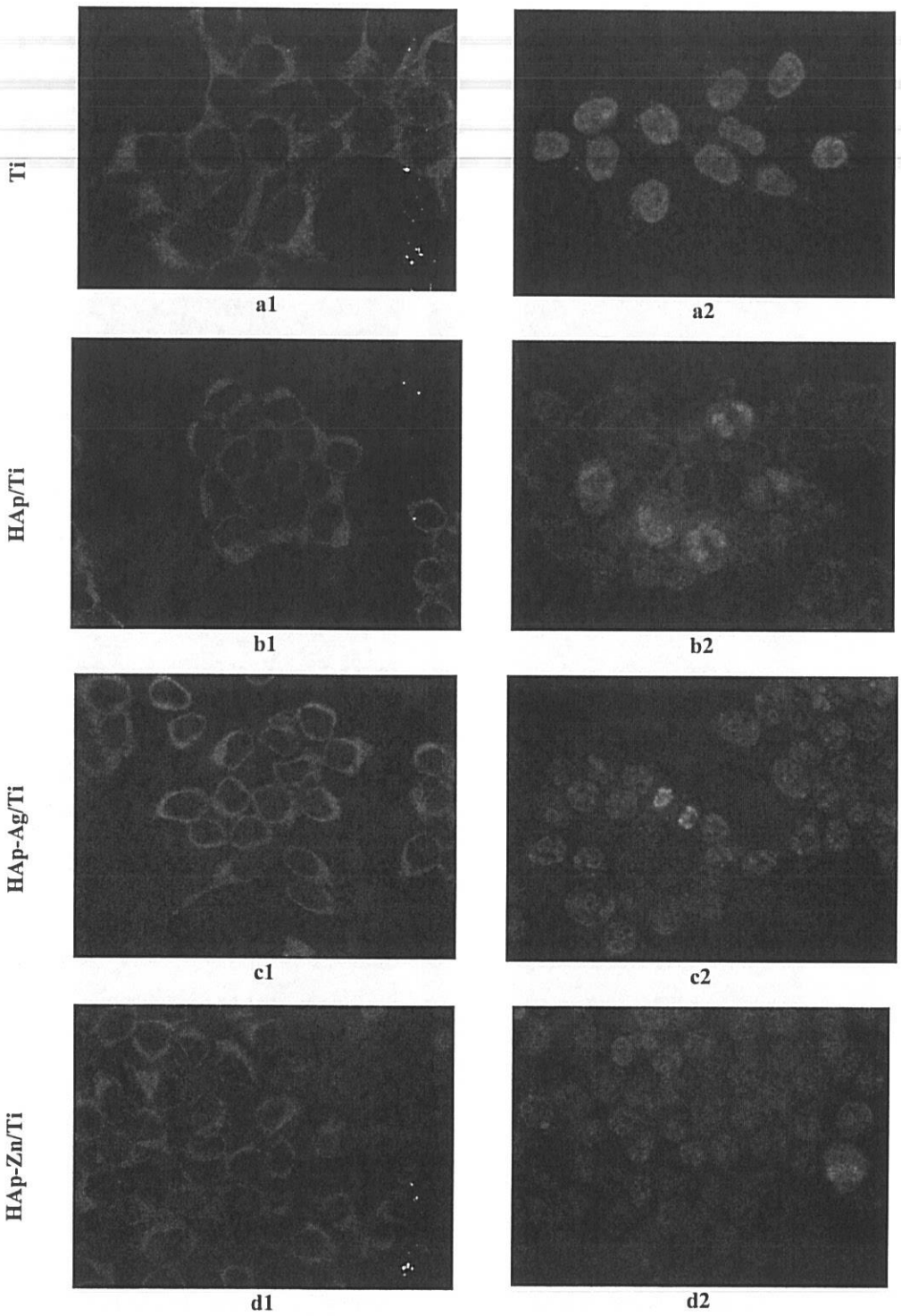


**Figure 3.19 a - Staining for PDI of the coating at magnification ×63 (a1, b1, c1, d1)**

**Figure 3.19 b - Staining for Ki67 of the coating at magnification ×63 (a2, b2, c2, d2)**

+ Cell proliferation

| Days | Ti ($\times 10^4$) | HAp/Ti ($\times 10^4$) | HAp-Ag/Ti ($\times 10^4$) | HAp-Zn/Ti ($\times 10^4$) | Control ($\times 10^4$) |
|---|---|---|---|---|---|
| 1 | 56.625 | 64.625 | 78.125 | 78.875 | 99 |
| 3 | 128.75 | 173.375 | 252.5 | 279.75 | 506.75 |
| 4 | 529.125 | 565.25 | 687 | 694.25 | 1526.625 |

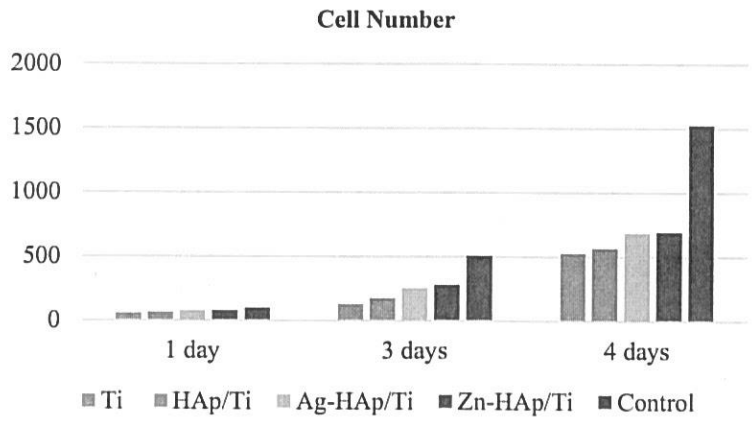


**Fig 3.20 - The number of cells on the coating after 1, 3 and 4 days.**

| Days | Ti (%) | HAp/Ti (%) | HAp-Ag/Ti (%) | HAp-Zn/Ti (%) | Control (%) |
|---|---|---|---|---|---|
| 1 | 77.73555 | 80.65162 | 83.10838 | 85.61191 | 88.29663 |
| 3 | 81.87358 | 84.37174 | 85.95683 | 86.34199 | 88.38133 |
| 4 | 82.09835 | 85.14409 | 86.19814 | 86.41666 | 89.15922 |

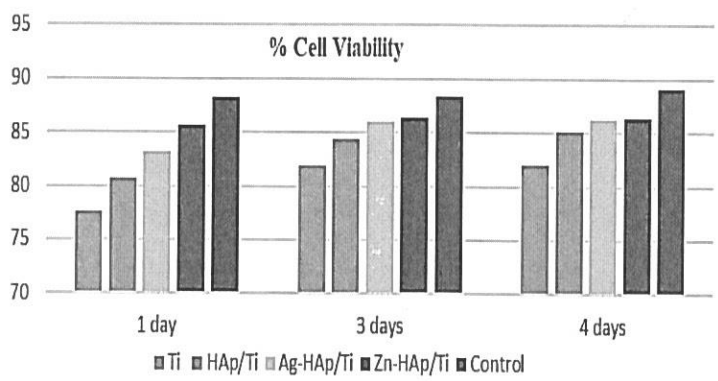


**Fig 3.21 - Cell Viability of the coatings after 1, 3 and 4 day**

# Chapter 4: Conclusions and orientations of future work

## 4.1 Conclusions

There are a lot of coating methodologies like deposition: plasma spray deposition, sol–gel derived coatings, pulsed laser physical vapor deposition, ED, ion beam assisted, magnetron sputtering, micro-arc oxidation, etc. In my present thesis, efforts are completed to display a summary of the basic principles of ED techniques. It contains the beneficial characterizations like bioactivity behavior and biocompatibility property related with these coatings for the surface modifications of Ti and Ti6Al4V.

The following conclusions are drawn aim to present my work in my thesis:

1. The Ca-P deposited coating on Ti6Al4V substrates by ED process was successfully formed. The uniform Ca-P coating cover all specimen substrate with micro-structure flake-like morphology, which stacking onto the surface of the Ti4Al6V substrate and creating uniformly clusters. The homogeneity of Ca-P coating was assessed using the Ca/Ti molar ratio, which ranged from 0.952 to 1.699 at the examined region of the coating surface that was revealed by SEM image.
2. ED process has been effectively applied for the achievement of un-doped HAp coatings and doped HAp-Ag coatings, which have antibacterial characteristic. The analytical data from XRD, SEM and EDX exhibited that this method is high beneficial in production of HAp coating. The HAp-Ag phase micro-structure and the XRD results exhibited that there are insignificant alterations on coating morphology at the regions on doped coating. The morphological characteristics of HAp have altered after $Ag^+$ ions doping, the surface with agglomeration of spherical particle of $Ag^+$ ions. Phase composition of HAp coatings changed by adding $Ag^+$ ions, the peaks have a litter moved towards left because of the substitution of $Ca^{+2}$ ions with $Ag^+$ in the HAp crystals.
3. HAp, HAp-Ag and HAp-Zn coatings were covered effectively onto a Ti surface by an ED technique at temperatures around 75°C, low current densities (0.6 $mA/cm^2$) and 20 min time. Uniform and thick coatings were obtained. Surface roughness was found to be reduced after adding Ag and Zn elements to the HAp coating (specifically, Ra = 1847.36 nm for HAp/Ti, Ra = 482.84 nm for HAp-Ag/Ti, Ra = 214.79 nm for HAp-Zn/Ti). The thickness of the coating also decreased after adding Ag and Zn elements (specifically, HAp/Ti (12.73), HAp-Ag/Ti (10.60), HAp-Zn/Ti (6.20). The thickness differences can be associated with the deposition rate which is influenced by the doping element, Ag or Zn, added in the electrolyte. Considering that all the parameters involved in the

electrochemical deposition were maintained constant, it can be assumed that the doping elements affects the deposition rate and/or HAp nucleation and growth.

4. The morphology of HAp was made of thin ribbon like crystals; the addition of Ag into HAp didn't induce major modification of the ribbon like morphology, but some Ag particle agglomerations were noted; in the case of HAp-Zn coatings, the morphology was made of very thin crystals which formed an interconnected porous network. After the period of 21 days of immersion in SBF solution the highest values were registered for HAp-Ag coatings (7.11 mg), followed by HAp (4.58 mg) and HAp-Zn (4.38 mg), while the cp-Ti have registered the smallest value (2.11 mg). The preliminary cell culture investigations exhibited that Ag-HAp and Zn-HAp coatings were non-cytotoxic and biocompatible and overall addition of Ag and Zn into HAp enhanced the behavior of HAp. Even though both doped coatings have improved the corrosion resistance of the cp-Ti substrate and the electrochemical behavior of HAp, it is worth mentioning that the smallest corrosion current density and highest polarization resistance was obtained for the HAp-Zn coatings, closely followed by the ones in which Ag was used as doping element.

**4.2 Personal contributions**

- The thesis has successfully contributed to the modification of Titanium and Ti6Al4V surface by adding two elements silver and zinc to hydroxyapatites coating through electrochemical deposition method (Ag-HAp coatings and Zn-HAp coatings). The obtained results meet the requirements of the surface for biomedical materials such as the uniformity of the coatings, the properties of biological activity, the biocompatibility, and the ability to resist corrosion;

- The thesis also contributes to the successful construction of the parameters of the electrochemical deposition method, which create the biomedical material surfaces to overcome the initial disadvantages of Titanium and Ti6Al4V such as: poor biocompatibility, low bioactivity; while enhancing the corrosion resistance, and exhibiting the non-toxic properties;

- With the parameters of electrochemical deposition built up, the findings on the morphology of coatings were mentioned:

+ Indeed, the addition Zn and Ag cause to transform in the morphology of HAp coatings onto Ti specimens. The significant differences of morphologies on the surface of found HAp, HAp-Ag and HAp-Zn coatings with plate-like crystals, plate-like crystals combined with white flowering branches-like crystals and interconnected network-type structure, respectively.

+ The morphology of HAp was made of thin ribbon like crystals; the addition of Ag into HAp didn't induce major modification of the ribbon like morphology, but some Ag particle agglomerations were noted; in the case of HAp-Zn coatings, the morphology was made of very thin crystals which formed an interconnected porous network, suggesting that Zn alters the nucleation kinetics;

- The elemental composition indicated that the addition of Ag and Zn enhances the Ca/P ratio of HAp. The thesis also contributes in the discoveries of atomic composition: the addition of Ag and Zn enhances the Ca/P ratio of HAp. The HAp-Ag/Ti, HAp-Zn/Ti coatings with a richer Ca/P ratio than HAp coating.

- The phase findings of the Ag-HAp phase micro-structure: phase composition also changed by addition of $Ag^{+}$ ions, the peaks have slightly moved towards left because of the substitution of $Ag^{+}$ ions for $Ca^{+2}$ in the HAp lattice;

- The aspects of the surface roughness and the thickness were also mentioned: the surface roughness was found to be reduced after adding Ag and Zn elements to the HAp coating, while the thickness of the coating also decreased after adding Ag and Zn elements;

- Detection of the coating's corrosion resistance: the both doped coatings (Ag-HAp coatings and Zn-HAp coatings) have improved the corrosion resistance of the cp-Ti substrate and the electrochemical behavior of HAp;

- Additionally, the *in vitro* test show that Ag-HAp and Zn-HAp coatings were non-cytotoxic and biocompatible.

In summary, the thesis has made a significant contribution in the modification of the Ti and Ti6Al4V surface. Since then, the thesis will have directions for development and expansion in the near future.

### 4.3 Orientation of future work

Based on the theoretical and experimental studies that have been done to reveal several promising avenues of future work:

- Further improvement through studies on the Ag and Zn co-doped HAp coating (HAp-Ag-Zn coating) by the electrochemical deposition technique. The influence of co-doped HAp coating on the aspect such as mechanical properties, physicochemical properties of HAp. Also, the co-doped HAp coating will be characterized further in terms of its crystallographic structure, thickness, adhesion, etc.

- Next works will be concentrated to investigate the coatings produced by the antibacterial characterizations of coatings on Ti and Ti6Al4V.

## *Bibliography references (selection)*


[1] Yajing Yan, Xuejiao Zhang, Huanhuan Mao, Yong Huang, Qiongqiong Ding, Xiaofeng Pang, Hydroxyapatite-gelatin functionalized graphene oxide composite coatings deposited on TiO2 nanotube by electrochemical deposition for bio-medical applications, Applied Surface Science 329 (2015),, 76–82

[2] Yongxiang Zeng, Xibo Pei, Shuying Yang, Han Qin, He Cai, Shanshan Hu, Lei Sui, Qianbing Wan, Jian Wang, Graphene oxide-hydroxyapatite composite coatings fabricated by electrochemical deposition, Surface & Coatings Technology, (2015),

[3] Yajing Yan, Xuejiao Zhang, Caixia Li, Yong Huang, Qiongqiong Ding, Xiaofeng Pang, Preparation, and characterization of chitosan-silver-hydroxyapatite composite coatings onTiO2 nanotube for bio-medical applications, Applied Surface Science 332, 62–69, (2015)

[4] Yajing Yan, Qiongqiong Ding, Yong Huang, Shuguang Han, Xiaofeng Pang, Magnesium substituted hydroxyapatite coating on titanium with nanotublar TiO2 intermediate layer via electrochemical deposition, Applied Surface Science 305, 77–85, (2014),

[5] Xibo Pei Yongxiang Zeng Rui He Zhongjie Li Lingyang Tian Jian Wang Qianbing Wan Xiaoyu Li Hong Bao, Single-walled carbon nanotubes-hydroxyapatite coatings on titanium obtained by electrochemical deposition, Applied Surface Science, (2014).

[6] Kang Lee, Yong-Hoon Jeong, Yeong-Mu Ko, Han-Cheol Choe, William A. Brantley, Hydroxyapatite coating on micropore-formed titanium alloy utilizing electrochemical deposition, Thin Solid Film, (2013)

[7] M.A. El Mhammedi, M. Achak, M. Bakasse, Evaluation of a platinum electrode modified with hydroxyapatite in the lead (II) determination in a square wave voltammetric procedure, Arabian Journal of Chemistry 6, 299–305, (2013).

[8] D. Gopi, E. Shinyjoy, M. Sekar, M. Surendiran, L. Kavitha, T.S. Sampath Kumar, Development of carbon nanotubes reinforced hydroxyapatite composite coatings on titanium by electrodeposition method, Corrosion Science 73, 321–330, (2013).

[9] Nik Norziehana Che Isa, Yusairie Mohd and Norjanah Yury, (2012), Electrochemical Deposition and Characterization of Hydroxyapatite (HAP) on Titanium Substrate, APCBEE Procedia 3, 46 – 52, (2012)

[10] D.J. Blackwood, K.H.W. Seah, Galvanostatic pulse deposition of hydroxyapatite for adhesion to titanium for bio-medical purposes, Materials Science and Engineering C 30 561–565, (2010).

[11] D.J. Blackwood, K.H.W. Seah, Electrochemical cathodic deposition of hydroxyapatite -Improvements in adhesion and crystallinity, Materials Science and Engineering C 29, 1233–1238, (2009).

[12] Jian Wang, Yonglie Chao, Qianbing Wan, Zhimin Zhu, Haiyang Yu, Fluoridated hydroxyapatite coatings on titanium obtained by electrochemical deposition, Acta Biomaterialia 5, 1798–180, (2009)

[13] Zhao Xuhui, Yang Lingfang, Zuo Yu and Xiong Jinping, Hydroxyapatite Coatings on Titanium Prepared by Electrodeposition in a Modified Simulated Body Fluid, Chinese Journal of Chemical Engineering, 17(4) 667- 671, (2009)

[14] Ming-[28]Jie Jiao, Xiao-Xiang Wang, Electrolytic deposition of magnesium-substituted hydroxyapatite crystals on titani[29]um substrate, Materials Letters 63, 2286–2289, (2009)

[15] Dai-Hua He,30] Pu Wang, Ping Liu, Xin-Kuan Liu, Feng-Cang Ma, Jun Zhao, HA coating fabricated by electrochemical deposition on modified Ti6Al4V alloy, Surface & Coatings Technology, (2015)

[16] D. Gopi, El-Sayed M. Sherif, D. Rajeswari, L. Kavitha, R. Pramod, Jishnu Dwivedi, S.R. Polaki, Evaluation of the mechanical and corrosion protection performance of electrodeposited hydroxyapatite on the high energy electron beam treated titanium alloy, Journal of Alloys and Compounds 616, 498–504, (2014)

[17] Lidia Benea, Eliza Mardare-Danaila, Jean-Pierre Celis, Increasing the tribological performances of Ti–6Al–4V alloy by forming a thin nanoporous TiO2 layer and hydroxyapatite electrodeposition under lubricated conditions, Tribology International 78, 168–175

[18] N. Metoki, L. Leifenberg-Kuznits, W. Kopelovich, L. Burstein, M. Gozin, N. Eliaz, Hydroxyapatite coatings electrodeposited at near-physiological conditions, Materials Letters 119, 24–27, (2014)

[19] Dhanaraj Gopi, Arumugam Karthika, Subramani Nithiya, Louis Kavitha, In vitro biological performance of minerals substituted hydroxyapatite coating by pulsed electrodeposition method, Materials Chemistry and Physics 144, 75 – 85, (2014).

[20] M. Saremi and B. Mottaghi Golshan, Electrodeposition of nano size hydroxyapatite coating on Ti alloy, Iranian Journal of Materials Science and Engineering, Vol. 3, Numbers 3 and 4, Summer and Autumn 2006

[21] R. Drevet, H. Benhayounea, L. Worthama, S. Potirona, J. Dougladeb, D.L. Maquina, Effects of pulsed current and H2O2 amount on the composition of electrodeposited calcium phosphate coatings, Mater. Charact. 61 (2010), 786-795

[22] T. Frade, V. Bouzon, A. Gomes, M.I.S. Pereira, Pulsed-reverse current electro-deposition of Zn and Zn-TiO2 nanocomposite films, Surf. Coat. Technol. 204 (2010), 3592-3598

[23] H. Adelkhani, M.R. Arshadi, J. Alloys Compd. Properties of Fe–Ni–Cr alloy coatings by using direct and pulse current electro-deposition, 476 (2009) 234-237

[24] R. Drevet, H. Benhayoune, Pulsed electro-deposition for the synthesis of strontium-substituted calcium phosphate coatings with improved dissolution properties, Mater. Sci. Eng. C 33 (2013) 4260-4265

[25] V. Sergo, O. Sbaizero, D.R. Clarke, Mechanical and chemical consequences of the residual stresses in plasma sprayed hydroxyapatite coatings, Biomaterials, 18 (1997), p. 477

[26] Yajing Yan, Xuejiao Zhang, Yong Huang, Qiongqiong Ding, Xiaofeng Pang, Antibacterial and bioactivity of silver substituted hydroxyapatite/TiO2 nanotube composite coatings on titanium, Applied Surface Science 314 (2014) 348–357

[27] Xiong Lu, Bailin Zhang, Yingbo Wang, Xianli Zhou, Jie Weng, Shuxin Qu, Bo Feng, Fumio Watari, Yonghui Ding and Yang Leng, Nano-Ag-loaded hydroxyapatite coatings on titanium surfaces by electrochemical deposition J. R. Soc. Interface (2011) 8, 529–539

[28] F. Ren, R. Xin, X. Ge, Y. Leng, Characterization and structural analysis of zinc substituted hydroxyapatites, Acta Biomater. 5 (2009) 3141–3149

[29] Y. Tang, H.F. CHAppell, M.T.Dove, R.J.Reeder, Y.J.Lee, Zinc incorporation into hydroxylapatite, Biomaterials 30(2009) 2864–2872

[30] H. Hu, W. Zhang, Y. Qiao, X. Jiang, X. Liu, C. Ding, Antibacterial activity, and increased bone marrow stem cell functions of Zn-incorporated TiO2 coatings on titanium, Acta Biomaterialia 8 (2012) 904–915

[31] Zhen Geng, Zhenduo Cui, Zhaoyang Li, Shengli Zhu, Yanqin Liang, Yunde Liu, Xue Li, Xin He, Xiaoxu Yu, Renfeng Wang, Xianjin Yang, Strontium incorporation to optimize the antibacterial and biological characteristics of silver-substituted hydroxyapatite coating, Materials Science and Engineering C 58 (2016) 467–477

[32] Andrea Ewald, Daniel Hösel, Sarika Patel, Liam M. Grover, Jake E. Barralet, Uwe Gbureck, Silver-doped calcium phosphate cements with antimicrobial activity, Acta Biomaterialia 7 (2011) 4064–4070

[33] Jinhua Li, Xuanyong Liu, Yuqin Qiao, Hongqin Zhu, Chuanxian Ding, Antimicrobial activity and cytocompatibility of Ag plasma-modified hierarchical TiO2 film on titanium surface, Colloids and Surfaces B: Biointerfaces 113 (2014) 134–145

[34] Chao-Ming Xie, Xiong Lu, Ke-Feng Wang, Fan-Zhi Meng, Ou Jiang, Hong-Ping Zhang, Wei Zhi, and Li-Ming Fang, Silver Nanoparticles and Growt.h Factors Incorporated Hydroxyapatite Coatings on Metallic Implant Surfaces for Enhancement of Osteo-inductivity and Antibacterial Properties, Applied materials & Interfaces

[35] Buddy D. Ratner, 'The Biocompatibility of Implant Materials', Host Response to Biomaterials, the Impact of Host Response on Biomaterial Selection 2015, Pages 37–51.

[36] Chao Shi, Jianyong Gao, Ming Wang, Jingke Fu, Dalin Wang, Yingchun Zhu, Ultra-trace silver-doped hydroxyapatite with non-cytotoxicity and effective antibacterial activity, Materials Science and Engineering C 55 (2015) 497–505

[37] D.M. Vraceanu, **T. Tran**, E. Ungureanu, V. Negoiescu, M. Tarcolea, M. Dinu, A. Vladescu, C.M. Cotrut, Pulsed electrochemical deposition of Ag doped hydroxyapatite bio-active coatings on Ti6Al4V for medical purposes, Scientific Bulletin U.P.B 2018, Series B - Chemistry and Materials Science, Vol. 80, Iss.1, pp. 173 – 184

[38] **Tran Thi Thanh**, Cosmin Mihai COTRUT, Maria Diana VRANCEANU, Elena UNGUREANU, Mihai TARCOLEA, Studies of micro-structure and composition of the modified HAp coating via SEM investigations, Scientific Bulletin U.P.B 2020, Series B - Chemistry and Materials Science, Vol. 82, Iss.1, pp. 145 – 154

[39] **Thi Thanh TRAN**, Norica Beatrice NICHITA, Mihaela-Olivia DOBRICA, Cosmin Mihai COTRUT, Maria Diana VRANCEANU, Mihai TARCOLEA, In vitro biocompatibility investigation of silver and zinc modified hydroxyapatite deposited on implant materials, Scientific Bulletin U.P.B 2020, Series B - Chemistry and Materials Science, Vol. 82, Iss.3, pp. 231 – 248